Blockade of EGFR and MEK Intercepts Heterogeneous Mechanisms of Acquired Resistance to Anti-EGFR Therapies in Colorectal Cancer

(Article begins on next page)

25 November 2024

UNIVERSITÀ DEGLI STUDI DI TORINO

This is an author version of the contribution published on:

Blockade of EGFR and MEK intercepts heterogeneous mechanisms of acquired resistance to anti-EGFR therapies in colorectal cancer

Sandra Misale[1,2*], Sabrina Arena[1,2*], Simona Lamba[1,2], Giulia Siravegna[1,2], Alice Lallo[1,2], Sebastijan Hobor[2], Mariangela Russo[1,2], Michela Buscarino[2], Luca Lazzari[2,3], Andrea Sartore Bianchi[4], Katia Bencardino[4], Alessio Amatu[4], Calogero Lauricella[5], Emanuele Valtorta[5], Salvatore Siena[4], Federica Di Nicolantonio[1,2] and Alberto Bardelli[1,2,3†]

[1] University of Torino, Department of Oncology, 10060 Candiolo, Torino, Italy [2] IRCC, Institute for Cancer Research and Treatment at Candiolo, Torino, Italy [3] FIRC Institute of Molecular Oncology (IFOM), Milano, Italy [4] Falck Division of Medical Oncology, [5] Division of Pathology, Niguarda Cancer Center, Ospedale Niguarda Ca' Granda, 20162 Milano , Italy

*These authors contributed equally to this work

†To whom correspondence should be addressed. E-mail: alberto.bardelli@unito.it

Abstract

Colorectal cancers (CRC) that are sensitive to the anti EGFR antibodies cetuximab or panitumumab almost always develop resistance within several months of initiating therapy. We report the emergence of polyclonal KRAS, NRAS and BRAF mutations in CRC cells with acquired resistance to EGFR blockade. Regardless of the genetic alterations, resistant cells consistently displayed MEK and ERK activation, which persisted after EGFR blockade. Inhibition of MEK1/2 alone failed to impair the growth of resistant cells in vitro and in vivo. An RNA interference screen demonstrated that suppression of EGFR together with silencing of MEK1/2 was required to hamper the proliferation of resistant cells. Indeed, concomitant pharmacological blockade of MEK and EGFR induced prolonged ERK inhibition and severely impaired the growth of resistant tumor cells. Heterogeneous and concomitant mutations in KRAS and NRAS were also detected in plasma samples from patients who developed resistance to anti-EGFR antibodies. A mouse xeno-transplant from a CRC patient who responded and subsequently relapsed upon EGFR therapy showed exquisite sensitivity to combinatorial treatment with MEK and EGFR inhibitors. Collectively, these results identify genetically distinct mechanisms that mediate secondary resistance to anti-EGFR therapies, all of which reactivate ERK signaling. These observations provide a rational strategy to overcome the multifaceted clonal heterogeneity that emerges when tumors are treated with targeted agents. We propose that MEK inhibitors, in combination with cetuximab or panitumumab, should be tested in CRC patients who become refractory to anti-EGFR therapies.

Introduction

The development of secondary (acquired) resistance is a common feature of anticancer treatment. The identification of mechanisms underlying secondary resistance can lead to rational development of additional lines of therapy. However, recent evidence indicates that a variety of resistance mechanisms to targeted drugs can emerge. When BRAF mutant melanomas are exposed to BRAF inhibitors, surviving cells display NRAS, MEK1/2 or COT mutations, PDGFRB overexpression, BRAF gene amplification or expression of BRAF truncated forms (*1-5*). Similarly, lung cancers carrying EGFR mutations escape treatment with the highly specific inhibitors erlotinib and gefitinib, through EGFR secondary mutations (T790M), MET amplification, HER2 amplification, MAPK1 amplification, PIK3CA mutations, AXL up-regulation and other mechanisms (*6-12*).

These discoveries suggest that every patient with a malignancy that becomes refractory to a targeted therapy should ideally undergo a tumor biopsy, allowing the assessment of the mechanism(s) of resistance through extensive costly molecular analyses. Even if this level of sophistication could be eventually achieved in the clinical setting, advanced stage patients often have multiple metastatic lesions in different organs. It is likely that the biopsied lesion would not be representative of the heterogeneity of the entire disease burden at relapse (*13*).

The realization that relapsed tumors are highly molecularly heterogeneous poses a formidable therapeutic challenge, as it would seem quite difficult to overcome the multiple resistance mutations that arise in individual patients. We hypothesized that the plethora of molecular determinants causative of secondary resistance would ultimately converge downstream in the signaling cascade, at a limited number of critical points.

In order to test this assumption, we studied secondary resistance to the monoclonal antibodies cetuximab and panitumumab. These drugs are mostly effective in colorectal cancer (CRC) patients who do not carry mutations in KRAS, NRAS or BRAF (*14, 15*). In these individuals, response to EGFR blockade can result in remarkable tumor regressions, but these are short lived (*16*) and progression occurs within months (*17*).

We initially identified several cell lines with molecular features representing a subset of patients who respond to cetuximab and/or panitumumab. These were then treated with anti-EGFR antibodies until resistant derivatives emerged. In accordance with our recent report, resistant cells frequently displayed KRAS mutations (*18*). We noted, however, that the resistant cell population was heterogeneous, and not all cells carried KRAS mutations. This phenomenon is reminiscent of what we and others have found in clinical samples from patients who respond and then progress upon treatment with cetuximab or panitumumab (*18, 19*). This prompted us to define additional mechanisms of resistance to EGFR blockade and to assess the pathway they control, as this is a prerequisite to overcome acquired resistance.

Results

Distinct genetic events drive acquired resistance to anti-EGFR therapy in CRC cells

To generate models of acquired resistance to anti-EGFR targeted therapies, we took advantage of a panel of CRC cell lines that we found to be highly sensitive to cetuximab and/or panitumumab. These included DiFi, LIM1215, HCA-46, NCIH508 and OXCO-2 cells. Mutational profiling showed that these cell lines are wild type for KRAS (exons 2, 3, 4), NRAS (exons 2, 3), HRAS (exons 2, 3), BRAF (exon 15), and PIK3CA (exons 9, 20), with the exception of NCIH508 which carries a PIK3CA exon 9 mutation (p.E545K). These findings in cell lines are consistent with the clinical observations about the genetic status of CRC patients most likely to respond to cetuximab and panitumumab (*20, 21*).

Cells were exposed to cetuximab or panitumumab until resistant populations emerged. Derivative cells resistant to cetuximab (referred to as R-cetux) or panitumumab (which we called R-panit) displayed cross-resistance to both monoclonal antibodies, consistent with what has been reported in patients treated with panitumumab after previous cetuximab-based treatment (*22*)(Figure 1A).

In order to define the molecular mechanisms underlying acquired resistance, we initially performed Sanger sequencing of candidate genes, which are known to confer primary resistance to EGFR blockade in CRC (*20*). These included KRAS, BRAF, NRAS, and PIK3CA. Mutational profiling of the resistant populations revealed molecular alterations in KRAS, BRAF and NRAS, but not in PIK3CA (Fig.1B). OXCO-2 and LIM1215 resistant populations contained multiple mutations. Most of the changes affected residues known to activate the corresponding protein, such as KRAS position 12, BRAF position 600 and NRAS positions 12 and 61 (Fig.1B and Fig. S1 A-B). A recent study indicated that CRC tumors resistant to cetuximab may acquire a secondary mutation in the extracellular domain of EGFR (S492R), which would prevent drug binding (*23*). Sequencing of the EGFR ectodomain in genomic DNA and cDNA obtained from resistant clones ruled out the presence of this mutation. Previous reports showed that gene amplification of KRAS, HER2 or MET can also confer resistance to anti-EGFR targeted therapies (*18, 24-27*). To assess whether gene copy variations could have emerged during drug selection, real-time quantitative PCR was performed on the same panel of candidates. This analysis revealed amplification of KRAS in DiFi R-cetux, HCA-46 R1-cetux and NCIH508 R-cetux and to a lesser extent in NCIH508 R-panit cell lines. Amplification of the MET or HER2 genes was not observed (Fig S2 A-B). We did not detect an increase in KRAS gene copy number in any of the parental lines. However, we previously reported that very rare cells in the DiFi population display KRAS overexpression by immunohistochemical analysis (*18*). We cannot exclude that a few KRAS-amplified cells (below the limit of detection of the RT-PCR assay) also exist in the other parental cell lines. To further address this aspect, we performed IHC (with KRAS antibodies) and FISH analysis (with a KRAS gene probe) of HCA-46 and NCIH508 parental and resistant cell populations. IHC and FISH confirmed the presence of KRAS-amplified cells in the resistant population and indicated that the

parental cells do not display this molecular alteration (Fig S3 A-B).

To formally assess whether different genetic alterations occurred in a mutually exclusive pattern, we cloned the populations of resistant cells. We found that single colonies could not be efficiently isolated from HCA-46 and NCIH508 cell lines. We therefore focused on LIM1215 R1-cetux, LIM1215 R2-cetux, and OXCO-2 R1-cetux cells, which proved capable of generating individual clones upon limiting dilution. All LIM1215 R2-cetux derivative clones (70/70) carried the KRAS G13D mutation, confirming that the resistant population was homogeneous. On the contrary, out of 13 clones derived from LIM1215 R1-cetux, 4 carried the KRAS G12R, 4 displayed the KRAS K117N variant (*28*) and the remaining 5 clones carried the NRAS G12C mutation. OXCO-2 R-cetux derived clones (66 clones in total) showed either KRAS G13D (42 clones) or BRAF V600E mutations (24 clones). To obtain more accurate quantification of the percentage at which each allele was present in the resistant populations, we performed BEAMing analysis on a subset of the resistant derivatives (Table S1).

The resistance protocol was then repeated starting from an independent batch of parental cells (LIM1215, OXCO-2, HCA-46) to assess the reproducibility of the approach and to evaluate the emergence of additional variants. LIM1215 R4-cetux again displayed a mixed population of KRAS G13D and KRAS G12D. OXCO-2 R2-cetux contained NRAS G12C, G12D and G13D. HCA-46 R2--cetux displayed KRAS G13D mutation.

Overall these results suggest that: i) Multiple genetic mechanisms can drive resistance to EGFR blockade and ii) several sub-clones often coexist in the population which emerges after selection with anti-EGFR therapies.

Genetic alterations in EGFR signaling biochemically converge to activate MEK and ERK

As described above, escape from EGFR blockade in CRC cells is associated with the emergence of distinct alterations in several genes. We hypothesized that the plethora of molecular determinants causative of acquired drug resistance would ultimately converge at a limited number of signaling switches which, in turn, could be rationally targeted by further lines of therapy. To test this assumption, we performed biochemical analysis of the resistant derivatives. For these studies, we elected to use LIM1215 R-panit (KRAS G13D, NRAS G12C), OXCO-2 R1-cetux (KRAS G12D, BRAF V600E), HCA46 R-panit (KRAS G12C) and NCIH508 R-cetux (KRAS amplified), because they are representative of the distinct resistance mechanisms which emerged upon selection with cetuximab and panitumumab (Fig. 1B). We started by assessing levels of RAS activation using a CRAF pull down assay. We found that resistant cells displayed increased GTP-bound KRAS as compared to the matched parental cells (Fig. S4). We next assessed the phosphorylation status of EGFR and its downstream effectors MEK and ERK by Western blot analysis. We found that MEK and/or ERK were consistently activated in resistant cells as compared to their parental counterparts (Fig. 2 A, B, C and D). Of relevance, sustained MEK or ERK activation was present in the resistant derivatives independent of the genetic mechanism of

resistance. These results revealed that CRC cells become refractory to anti-EGFR therapies by increasing signaling output through the MEK-ERK pathway.

Resistant cells are sensitive to concomitant silencing of the EGFR and MEK1/2 genes

We assessed whether the genetic alterations associated with the emergence of resistance to anti-EGFR drugs might underlie functional dependencies, which could be exploited to design therapeutic strategies for tumors with secondary resistance to cetuximab and panitumumab.

As a first step, we employed a siRNA mediated functional screening to identify genes that alone or in combination could suppress the growth of resistant cells. The RNA interference assay was devised to interrogate candidate genes known to be involved in resistance to cetuximab or panitumumab and/or effectors of EGFR-initiated signaling. These included KRAS, NRAS, HRAS, BRAF, CRAF, MEK1/2, HER2, HER3, PIK3CA and AKT1 (Fig. 3A). To confirm the specificity and the efficacy of the assays, siRNA-mediated suppression was followed by western blotting with antibodies against the individual targeted gene products. As shown in figure S5, individual siRNA effectively and specifically suppressed the designated target gene. The siRNA-mediated functional screen revealed that resistant cells were usually dependent upon the expression of the genes whose alterations emerged during the selection procedure. For example, KRAS mutant/amplified cells (LIM1215-R panit, HCA46-R panit and NCIH508R-cetux) were sensitive to KRAS suppression (Fig 3A). Of note, LIM1215 R-panit did not show growth impairment upon NRAS silencing despite harboring an NRAS mutation. This result is consistent with our observations that NRAS mutant cells are a minor sub-clone in the bulk population as assessed by BEAMing analysis (Table S1). OXCO-2 R1-cetux cells, which are a mixture of KRAS and BRAF mutant cells, were greatly sensitive to combined suppression of KRAS+BRAF (Fig. 3B). The finding that siRNA-mediated suppression of MEK1/2 only marginally affected the growth of resistant cells was unexpected. We therefore assessed whether pimasertib, a selective allosteric MEK inhibitor, which is being tested in clinical trials (*29, 30*), might have similar impact. Consistently with the result obtained by siRNA analysis, we found that pharmacological inhibition of MEK was unable to successfully block the growth of resistant cells (Fig. S6).

Resistance to EGFR blockade is reversed by concomitant inhibition of EGFR and MEK

We reasoned that dependencies due to activation of signaling pathways associated with drugs inhibiting the EGF receptor might become apparent only when the receptor itself was concomitantly targeted. To directly test this hypothesis, we performed siRNA-mediated suppression of signaling effectors in association with silencing of the EGF receptor. Concomitant silencing of EGFR and MEK1/2 was the only combination capable of reducing the survival fraction below 50% in all four cell models (Fig. 3B). Parallel experiments in which concomitant targeting of the EGFR and MEK was achieved by combining siRNA suppression and pharmacological treatment confirmed these results (Fig. S7).

The finding that cells that developed resistance to EGFR blockade display constitutive activation of MEK but are only modestly affected by MEK inhibition is intriguing. To study this further, we performed biochemical analyses in the presence of EGFR and MEK inhibitors (cetuximab and pimasertib, respectively) alone or in combination. To verify the kinetics of this effect, we performed time course pharmacological treatments. Notably, we found that in the absence of cetuximab the MEK inhibitor pimasertib leads to efficient phospho-ERK suppression. This is transient, however, and after a few hours ERK became phosphorylated again (Fig. 4). Concomitant with ERK reactivation we observed increased phosphorylation of EGFR. Phosphorylation of the receptor increased over time and was maximal after 6-12 hours depending on the cell model. When the same experiment was performed in the presence of cetuximab, EGFR phosphorylation was suppressed and this was accompanied by prolonged abrogation of ERK phosphorylation (Fig. 4). Importantly, these results are consistent across multiple cell models of acquired resistance to EGFR blockade, irrespectively of their mutational status.

Concomitant inhibition of EGFR and MEK1/2 with cetuximab and pimasertib was effective not only in transient cell growth experiments but also when the drugs were tested in long term proliferation assays (Fig. 5A). We next assessed the efficacy of the concomitant EGFR-MEK blockade in vivo. Pools of OXCO-2 and NCIH508 cetuximab-resistant cells were injected in nude mice. After tumors were established, mice were treated with vehicle, cetuximab and/or pimasertib alone, or the combination of the two agents. OXCO-2 R1-cetux tumors treated with cetuximab proliferated at a comparable rate to vehicle-treated xenografts. Pimasertib as a single agent delayed tumor growth without inducing regression. In contrast, the combination of cetuximab and pimasertib induced a remarkable reduction in tumor volume compared to baseline. Similar results were obtained in NCIH508 R-cetux xenografts (Fig. 5B and Table S2). Importantly, the two models confirmed that combinatorial treatment is effective in inducing tumor shrinkage in cetuximab-resistant cells irrespective of their mechanism of resistance.

Plasma samples from patients who develop resistance to EGFR blockade display KRAS and NRAS mutations

The cell-based findings suggested that upon EGFR blockade, multiple resistant clones emerge, and that resistance is often driven by genetically distinct mechanisms. In order to assess the clinical relevance of these findings, we examined samples from metastatic CRC patients who received anti-EGFR antibodies. We hypothesized that distinct genetic events would also be observed in samples (biopsies) from CRC patients who initially responded and then became refractory to either cetuximab or panitumumab. Needle biopsies are particularly difficult to obtain in this setting for a number of reasons, including the intrinsic risk of this invasive procedure (31). The scenario is further complicated by the fact that patients with metastatic CRC usually have multiple lesions. Therefore, biopsies represent only a snapshot of the overall disease and, accordingly, are not well suited to monitor the emergence of

resistant clones, which can be located in distant metastatic lesions. To overcome these limitations, at least in part, we have implemented a 'liquid biopsy' approach to analyze circulating free tumor DNA, because it is more likely to capture the overall genetic complexity of tumors in patients with advanced disease. We exploited the highly sensitive BEAMing technique to measure tumor-derived DNA mutations in the blood of patients (*18, 19, 32, 33*). We obtained plasma samples from 4 patients who responded and then became refractory to either cetuximab or panitumumab. BEAMing probes designed to identify the same somatic variants that were found in cell lines were used to monitor for KRAS, BRAF and NRAS mutations in plasma. Notably, in two cases (patients #1 and #2) multiple KRAS variants were detected at relapse but not at baseline, suggesting the emergence of several independent clones during treatment (Fig. 6A). In patient #2, the concomitant presence of KRAS and NRAS mutations was observed in the relapse sample (Fig. 6B). The same occurred at relapse in patient #3 (Fig 6C). In the last patient (#4), mutations in KRAS, NRAS and BRAF were not found at progression (the baseline plasma was not available for patients #3 and 4). These results suggest that therapy with anti-EGFR antibodies selects multiple clones carrying heterogeneous patterns of mutations, a situation akin with what we observed in preclinical models. Analogous results were obtained by Bettegowda and colleagues as described in the companion manuscript (*34*).

A patient-derived CRC xenograft with acquired resistance is sensitive to EGFR and MEK inhibition

Using an approach we previously optimized (*27*), we generated a mouse xeno-transplant (patient - derived xenograft, or PDX) from a lung metastasis of a CRC patient who responded and subsequently relapsed upon anti-EGFR therapy (cetuximab). This tumor carried a KRAS mutation (A146T) which is identical to one of the KRAS variants we found in LIM1215 R3-cetux cells (Fig.1B). After implantation and engraftment of the patient sample in a NOD-SCID mouse, the tumor was passaged and expanded for two generations. The morphological features of the biopsy obtained from the lung metastasis and a specimen from the xenotransplant grown in NOD-SCID mice were compared. As shown in Figure 6D, xenografted tumors retained the histopathological characteristics of their original patient counterpart. We also confirmed the presence of the KRAS mutation in the xenopatient by Sanger and BEAMing analysis. The xenografted tumor was serially transplanted until production of four cohorts, each consisting of 6 mice. These were randomized to vehicle alone, cetuximab monotherapy, pimasertib monotherapy and their combination. Notably, cetuximab or the MEK inhibitor pimasertib had limited effectiveness, while combinatorial (cetuximab-pimasertib) treatment prominently impaired tumor growth and induced moderate shrinkage (Fig. 6E ,S8 and Table S2).

Discussion

Recent evidence that cancer genomes (especially in the case of metastatic tumors) are highly heterogeneous (*13*) may explain why treatment with individual drugs (such as BRAF inhibitors or anti-EGFR antibodies) is only transiently effective. A cancer detectable by CT scanning contains billions of cells. Mathematical models indicate that in a single tumor mass (for example a CRC liver metastasis) there are hundreds to thousands of cells that are already resistant to a given targeted agent even before treatment is initiated (*19*). At first glance, overcoming resistance therefore appears to be an insurmountable task. We decided to focus on metastatic CRC (*35*) and the anti-EGFR monoclonal antibodies cetuximab and panitumumab as a model system to study how, at least in principle, this problem could be tackled. We reasoned that although alterations in multiple genes could confer resistance to EGFR blockade, their activation may ultimately converge downstream in the signaling pathway that was initially targeted (in this case the EGFR-MAPK pathway). Accordingly, this work was initiated based on two premises: i) tumors that develop resistance to EGFR blockade would be genetically heterogeneous and ii) activation of pathways conferring resistance would eventually converge on key downstream effector(s). Starting from several CRC cellular models that are highly sensitive to cetuximab and/or panitumumab, we obtained resistant derivatives by continuous drug exposure. In most cases, KRAS alterations (mutation or amplification) could be detected at resistance, in accordance with what has previously been reported (*18, 19*). Using several methodologies (sequencing and cloning), we found that the resistant populations were often highly heterogeneous and contained several KRAS alleles. Furthermore, we discovered that in addition to KRAS, NRAS and BRAF activating mutations could also be detected in several cellular models. This led us to postulate that the same might occur in patients. We reasoned that tissue biopsies would only offer a snapshot of the overall tumor mass, and might therefore be ill-suited to capture the multiclonal feature of the resistant disease. We therefore analyzed circulating free DNA, a form of liquid biopsy, which allows tumors to be genotyped using a blood sample from patients. Notably, we found that plasma samples of patients treated with anti-EGFR antibodies carried multiple distinct KRAS and NRAS alleles. These results, together with those described in a related manuscript in which circulating free DNA from patients treated with anti-EGFR antibodies was also analyzed (*34*), provide evidence that alterations in multiple genes are concomitantly associated with acquired resistance to EGFR blockade. The finding that within a single patient, resistance to EGFR blockade can be associated with mutations in several genes (such as KRAS and NRAS) underscores the molecular heterogeneity of resistant tumors. It should be acknowledged, however, that a large number of samples from resistant patients will be required to establish the prevalence and the extent of this phenomenon.

These results also highlight a striking overlap between genes that, when mutated, drive the so-called primary (de novo) resistance and those that allegedly sustain secondary (acquired) resistance. It was previously reported that alterations in KRAS, BRAF, NRAS, MET and HER2 can drive both de novo and acquired resistance (*17, 20, 24-27*). Both inter- and intra-patient tumor genetic heterogeneity have been observed, with the extent of the latter likely reflecting the point at which the alteration was acquired during tumorigenesis. For example, de novo KRAS mutations occur early during tumor progression, whereas the emergence of KRAS mutations upon EGFR targeting occurs when the tumor is treated (usually at the stage of metastatic disease). In this case the drug pressure is applied simultaneously, often to multiple metastases, which are genetically highly heterogeneous. Consequently, the spectrum of alleles driving secondary resistance appears evident even when only a few patients are examined. Overall, these results support the concept that primary and acquired resistances are driven by the same alterations.

We formulated the hypothesis that the molecular alterations emerging after treatment with a targeted agent would activate genes involved in the same pathway that was besieged by the selective pressure. We further assumed that the signals sustained by the mutant proteins would ultimately converge on a distinct downstream effector. Notably, these data mirror what was previously reported in cellular models and clinical samples of BRAF-mutant melanoma in which, independently of the mechanisms driving acquired resistance, reactivation of MAPK signaling is almost invariably detected (*36, 37*). Accordingly, clinical trials based on re-challenging melanomas with anti-MEK drugs have been designed (*38*). Collectively, biochemical analyses and reverse genetic experiments corroborate this hypothesis. We report that, regardless of the gene/mutation that confers resistance, the net output is invariably sustained activation (constitutive phosphorylation) of MEK and ERK, thus defining an example of convergent evolution. These data provide a rationale for overcoming resistance to EGFR antibodies using MEK inhibitors, many of which have already reached the clinic (*30*). Importantly, we found that blockade of MEK is not sufficient to inhibit the proliferation of resistant cells. Using siRNA screening and pharmacological treatments we found that cells which acquired resistance to cetuximab or panitumumab (through KRAS, BRAF or NRAS mutations) are dependent upon concomitant blockade of EGFR and MEK. Importantly, the requirement for EGFR-MEK concomitant blockade is evident not only *in vitro* but also *in vivo,* as shown by mouse xenograft experiments. Biochemical time course analysis showed that MEK inhibition leads to transient ERK inactivation, which is followed by phosphorylation of the receptor. The latter is blocked by the addition of cetuximab, thus explaining why the double hit (EGFR-MEK) is required. The mechanism of EGFR feedback activation after MEK blockade is reminiscent of what is observed when BRAF-mutant colorectal cancers are treated with BRAF or MEK inhibitors (*39*). Importantly, while our work suggests that MEK/ERK reactivation is linked to re-phosphorylation of the EGFR receptor, the moderate intensity of EGFR phosphorylation suggests that additional signaling routes may also contribute. To overcome the limits of our study, further investigations are needed to elucidate the precise biochemical players underlying the effectiveness of

the EGFR-MEK combination. However, the data generated in cell models were confirmed in a tumor xenograft derived from a patient who responded and then relapsed upon cetuximab therapy, thus supporting the clinical relevance of the findings.

Overall, the results presented in this manuscript define genetic alterations linked to secondary resistance to anti-EGFR monoclonal antibodies in preclinical models and CRC patients. Considering that in the clinical setting anti-EGFR antibodies are often used in combination with chemotherapy (*40, 41*), it will be of high interest to explore whether and to what extent treatment with chemotherapy affects the emergence of genetic alterations upon EGFR blockade. Thus, our study provides a rationale for clinical trials involving concomitant inhibition of EGFR and MEK in CRC patients who develop acquired resistance to cetuximab and panitumumab.

Materials and Methods

Study Design

This study was designed to define the mechanisms of acquired resistance to EGFR blockade in CRC and to define pharmacological strategies to overcome acquired resistance to cetuximab and panitumumab. In the first section of this study, CRC cell lines that developed acquired resistance to anti-EGFR therapies were molecularly characterized. In the second part, a subset of these cell models was analyzed at a biochemical level and with siRNA screening to identify signaling nodes that sustain resistance and can be pharmacologically targeted. Western blot analyses were performed at least twice, starting with independent cell lysates. SiRNA screening was performed using a pool of four different siRNAs for each target gene, and the results represent an average of three independent experiments. In the third section of the study, cell lines with acquired resistance to EGFR blockade were treated with drugs targeting proteins involved in signaling pathways. *In vitro* drug inhibition assays were performed in triplicates or quadruplicates. Cell lines were implanted in immunocompromised mice, which were then randomized to establish homogeneous treatment arms before drug administration. In the fifth section of the study we used the highly sensitive BEAMing technology to detect genetically heterogeneous KRAS and RAS mutations in plasma samples from four CRC patients who relapsed after anti-EGFR treatment. In the last section we established a tumor xenograft from a patient who relapsed after responding to EGFR blockade, which was then used to assess the combinatorial treatment initially tested in cell lines. The tumor sample was initially engrafted in one NOD-SCID mouse. After expansion in a large cohort of mice, xenografted tumors were randomized to establish homogeneous treatment arms for drug administration.

Statistical analysis

All data from the proliferation assay are presented as the mean ± SD of at least three independent experiments, each with three experimental replicates. SiRNA screenings are presented as the mean ± SD of three independent experiments, each with four experimental replicates. *In vivo* experimental data points represent mean ± SEM of the measurements of each mouse tumor.

List of Supplementary Materials

- Supplementary Materials and Methods
- Figure S1: Mutational profiling of candidate genes in resistant cells
- Figure S2: Gene copy analysis in resistant cells
- Figure S3: KRAS amplification in parental and resistant NCIH508 and HCA-46 cell lines
- Figure S4: Measurement of RAS activation in resistant cells.
- Figure S5: Biochemical validation of siRNA mediated gene knockdown
- Figure S6: Pharmacological inhibition of MEK in cells resistant to anti-EGFR blockade
- Figure S7: Pharmacological inhibition of EGFR or MEK1/2 with cetuximab or pimasertib.
- Figure S8: Sensitivity to combinatorial EGFR and MEK inhibition in a mouse xenograft from a metastatic CRC patient who relapsed after anti-EGFR therapy.
- Table S1:Frequencies of mutant alleles in resistant cell lines assessed by BEAMing.
- Table S2: Supplementary Excel file: tabular data for NCIH508 R-cetux and OXCO2 R1-cetux xenografts measurements and tabular data for PDX measurements.
- Table S3: List of Primers for gene amplification and sequencing
- Table S4: List of Primers and probes for BEAMing analysis
- Table S5: List of primers for gene copy number analysis by real-time PCR
- Table S6: List of siRNAs

References and Notes

1. R. Nazarian, H. Shi, Q. Wang, X. Kong, R. C. Koya, H. Lee, Z. Chen, M. K. Lee, N. Attar, H. Sazegar, T. Chodon, S. F. Nelson, G. McArthur, J. A. Sosman, A. Ribas, R. S. Lo, Melanomas acquire resistance to B-RAF(V600E) inhibition by RTK or N-RAS upregulation. Nature 468, 973-977 (2010)
2. C. M. Johannessen, J. S. Boehm, S. Y. Kim, S. R. Thomas, L. Wardwell, L. A. Johnson, C. M. Emery, N. Stransky, A. P. Cogdill, J. Barretina, G. Caponigro, H. Hieronymus, R. R. Murray, K. Salehi-Ashtiani, D. E. Hill, M. Vidal, J. J. Zhao, X. Yang, O. Alkan, S. Kim, J. L. Harris, C. J. Wilson, V. E. Myer, P. M. Finan, D. E. Root, T. M. Roberts, T. Golub, K. T. Flaherty, R. Dummer, B. L. Weber, W. R. Sellers, R. Schlegel, J. A. Wargo, W. C. Hahn, L. A. Garraway, COT drives resistance to RAF inhibition through MAP kinase pathway reactivation. Nature 468, 968-972 (2010)
3. P. I. Poulikakos, C. Zhang, G. Bollag, K. M. Shokat, N. Rosen, RAF inhibitors transactivate RAF dimers and ERK signalling in cells with wild-type BRAF. Nature 464, 427-430 (2010)
4. H. Shi, G. Moriceau, X. Kong, M. K. Lee, H. Lee, R. C. Koya, C. Ng, T. Chodon, R. A. Scolyer, K. B. Dahlman, J. A. Sosman, R. F. Kefford, G. V. Long, S. F. Nelson, A. Ribas, R. S. Lo, Melanoma whole-exome sequencing identifies (V600E)B-RAF amplification-mediated acquired B-RAF inhibitor resistance. Nat Commun 3, 724 (2012)
5. S. I. Nikolaev, D. Rimoldi, C. Iseli, A. Valsesia, D. Robyr, C. Gehrig, K. Harshman, M. Guipponi, O. Bukach, V. Zoete, O. Michielin, K. Muehlethaler, D. Speiser, J. S. Beckmann, I. Xenarios, T. D. Halazonetis, C. V. Jongeneel, B. J. Stevenson, S. E. Antonarakis, Exome sequencing identifies recurrent somatic MAP2K1 and MAP2K2 mutations in melanoma. Nat Genet 44, 133-139 (2012)
6. W. Pao, V. A. Miller, K. A. Politi, G. J. Riely, R. Somwar, M. F. Zakowski, M. G. Kris, H. Varmus, Acquired resistance of lung adenocarcinomas to gefitinib or erlotinib is associated with a second mutation in the EGFR kinase domain. PLoS Med 2, e73 (2005)
7. S. Kobayashi, T. J. Boggon, T. Dayaram, P. A. Janne, O. Kocher, M. Meyerson, B. E. Johnson, M. J. Eck, D. G. Tenen, B. Halmos, EGFR mutation and resistance of non-small-cell lung cancer to gefitinib. N Engl J Med 352, 786-792 (2005)
8. K. Takezawa, V. Pirazzoli, M. E. Arcila, C. A. Nebhan, X. Song, E. de Stanchina, K. Ohashi, Y. Y. Janjigian, P. J. Spitzler, M. A. Melnick, G. J. Riely, M. G. Kris, V. A. Miller, M. Ladanyi, K. Politi, W. Pao, HER2 amplification: a potential mechanism of acquired resistance to EGFR inhibition in EGFR-mutant lung cancers that lack the second-site EGFRT790M mutation. Cancer Discov 2, 922-933 (2012)
9. Z. Zhang, J. C. Lee, L. Lin, V. Olivas, V. Au, T. LaFramboise, M. Abdel-Rahman, X. Wang, A. D. Levine, J. K. Rho, Y. J. Choi, C. M. Choi, S. W. Kim, S. J. Jang, Y. S. Park, W. S. Kim, D. H. Lee, J. S. Lee, V. A. Miller, M. Arcila, M. Ladanyi, P. Moonsamy, C. Sawyers, T. J. Boggon, P. C. Ma, C. Costa, M. Taron, R. Rosell, B. Halmos, T. G. Bivona, Activation of the AXL kinase causes resistance to EGFR-targeted therapy in lung cancer. Nat Genet 44, 852-860 (2012)
10. D. Ercan, C. Xu, M. Yanagita, C. S. Monast, C. A. Pratilas, J. Montero, M. Butaney, T. Shimamura, L. Sholl, E. V. Ivanova, M. Tadi, A. Rogers, C. Repellin, M. Capelletti, O. Maertens, E. M. Goetz, A. Letai, L. A. Garraway, M. J. Lazzara, N. Rosen, N. S. Gray, K. K. Wong, P. A. Jänne, Reactivation of ERK Signaling Causes Resistance to EGFR Kinase Inhibitors. Cancer Discov 2, 934-947 (2012)
11. J. A. Engelman, K. Zejnullahu, T. Mitsudomi, Y. Song, C. Hyland, J. O. Park, N. Lindeman, C. M. Gale, X. Zhao, J. Christensen, T. Kosaka, A. J. Holmes, A. M. Rogers, F. Cappuzzo, T. Mok, C. Lee, B. E. Johnson, L. C. Cantley, P. A. Janne, MET amplification leads to gefitinib resistance in lung cancer by activating ERBB3 signaling. Science 316, 1039-1043 (2007)
12. L. V. Sequist, B. A. Waltman, D. Dias-Santagata, S. Digumarthy, A. B. Turke, P. Fidias, K. Bergethon, A. T. Shaw, S. Gettinger, A. K. Cosper, S. Akhavanfard, R. S. Heist, J. Temel, J. G. Christensen, J. C. Wain, T. J. Lynch, K. Vernovsky, E. J. Mark, M. Lanuti, A. J. Iafrate, M. Mino-Kenudson, J. A. Engelman, Genotypic and histological evolution of lung cancers acquiring resistance to EGFR inhibitors. Sci Transl Med 3, 75ra26 (2011)

13. M. Gerlinger, A. J. Rowan, S. Horswell, J. Larkin, D. Endesfelder, E. Gronroos, P. Martinez, N. Matthews, A. Stewart, P. Tarpey, I. Varela, B. Phillimore, S. Begum, N. Q. McDonald, A. Butler, D. Jones, K. Raine, C. Latimer, C. R. Santos, M. Nohadani, A. C. Eklund, B. Spencer-Dene, G. Clark, L. Pickering, G. Stamp, M. Gore, Z. Szallasi, J. Downward, P. A. Futreal, C. Swanton, Intratumor heterogeneity and branched evolution revealed by multiregion sequencing. N Engl J Med 366, 883-892 (2012)

14. A. H. Grossmann, W. S. Samowitz, Epidermal growth factor receptor pathway mutations and colorectal cancer therapy. Arch Pathol Lab Med 135, 1278-1282 (2011)

15. J. Y. Douillard, K. S. Oliner, S. Siena, J. Tabernero, R. Burkes, M. Barugel, Y. Humblet, G. Bodoky, D. Cunningham, J. Jassem, F. Rivera, I. Kocáková, P. Ruff, M. Błasińska-Morawiec, M. Šmakal, J. L. Canon, M. Rother, R. Williams, A. Rong, J. Wiezorek, R. Sidhu, S. D. Patterson, Panitumumab-FOLFOX4 treatment and RAS mutations in colorectal cancer. N Engl J Med 369, 1023-1034 (2013)

16. E. Van Cutsem, C. H. Kohne, E. Hitre, J. Zaluski, C. R. Chang Chien, A. Makhson, G. D'Haens, T. Pinter, R. Lim, G. Bodoky, J. K. Roh, G. Folprecht, P. Ruff, C. Stroh, S. Tejpar, M. Schlichting, J. Nippgen, P. Rougier, Cetuximab and chemotherapy as initial treatment for metastatic colorectal cancer. N Engl J Med 360, 1408-1417 (2009)

17. A. Bardelli, S. Siena, Molecular mechanisms of resistance to cetuximab and panitumumab in colorectal cancer. J Clin Oncol 28, 1254-1261 (2010)

18. S. Misale, R. Yaeger, S. Hobor, E. Scala, M. Janakiraman, D. Liska, E. Valtorta, R. Schiavo, M. Buscarino, G. Siravegna, K. Bencardino, A. Cercek, C. T. Chen, S. Veronese, C. Zanon, A. Sartore-Bianchi, M. Gambacorta, M. Gallicchio, E. Vakiani, V. Boscaro, E. Medico, M. Weiser, S. Siena, F. Di Nicolantonio, D. Solit, A. Bardelli, Emergence of KRAS mutations and acquired resistance to anti-EGFR therapy in colorectal cancer. Nature 486, 532-536 (2012)

19. L. A. Diaz, R. T. Williams, J. Wu, I. Kinde, J. R. Hecht, J. Berlin, B. Allen, I. Bozic, J. G. Reiter, M. A. Nowak, K. W. Kinzler, K. S. Oliner, B. Vogelstein, The molecular evolution of acquired resistance to targeted EGFR blockade in colorectal cancers. Nature 486, 537-540 (2012)

20. W. De Roock, B. Claes, D. Bernasconi, J. De Schutter, B. Biesmans, G. Fountzilas, K. T. Kalogeras, V. Kotoula, D. Papamichael, P. Laurent-Puig, F. Penault-Llorca, P. Rougier, B. Vincenzi, D. Santini, G. Tonini, F. Cappuzzo, M. Frattini, F. Molinari, P. Saletti, S. De Dosso, M. Martini, A. Bardelli, S. Siena, A. Sartore-Bianchi, J. Tabernero, T. Macarulla, F. Di Fiore, A. O. Gangloff, F. Ciardiello, P. Pfeiffer, C. Qvortrup, T. P. Hansen, E. Van Cutsem, H. Piessevaux, D. Lambrechts, M. Delorenzi, S. Tejpar, Effects of KRAS, BRAF, NRAS, and PIK3CA mutations on the efficacy of cetuximab plus chemotherapy in chemotherapy-refractory metastatic colorectal cancer: a retrospective consortium analysis. Lancet Oncol 11, 753-762 (2010)

21. M. Martini, L. Vecchione, S. Siena, S. Tejpar, A. Bardelli, Targeted therapies: how personal should we go? Nat Rev Clin Oncol 9, 87-97 (2012)

22. M. S. Banck, A. Grothey, Biomarkers of Resistance to Epidermal Growth Factor Receptor Monoclonal Antibodies in Patients with Metastatic Colorectal Cancer. Clin Cancer Res 15, 7492-7501 (2009)

23. C. Montagut, A. Dalmases, B. Bellosillo, M. Crespo, S. Pairet, M. Iglesias, M. Salido, M. Gallen, S. Marsters, S. P. Tsai, A. Minoche, S. Somasekar, S. Serrano, H. Himmelbauer, J. Bellmunt, A. Rovira, J. Settleman, F. Bosch, J. Albanell, Identification of a mutation in the extracellular domain of the Epidermal Growth Factor Receptor conferring cetuximab resistance in colorectal cancer. Nat Med 18, 221-223 (2012)

24. A. Bertotti, G. Migliardi, F. Galimi, F. Sassi, D. Torti, C. Isella, D. Corà, F. Di Nicolantonio, M. Buscarino, C. Petti, D. Ribero, N. Russolillo, A. Muratore, P. Massucco, A. Pisacane, L. Molinaro, E. Valtorta, A. Sartore-Bianchi, M. Risio, L. Capussotti, M. Gambacorta, S. Siena, E. Medico, A. Sapino, S. Marsoni, P. M. Comoglio, A. Bardelli, L. Trusolino, A molecularly annotated platform of patient-derived xenografts ("xenopatients") identifies HER2 as an effective therapeutic target in cetuximab-resistant colorectal cancer. Cancer Discov 1, 508-523 (2011)

25. K. Yonesaka, K. Zejnullahu, I. Okamoto, T. Satoh, F. Cappuzzo, J. Souglakos, D. Ercan, A. Rogers, M. Roncalli, M. Takeda, Y. Fujisaka, J. Philips, T. Shimizu, O. Maenishi, Y. Cho, J. Sun, A. Destro, K. Taira, K. Takeda, T. Okabe, J. Swanson, H. Itoh, M. Takada, E. Lifshits, K. Okuno, J. A. Engelman, R. A. Shivdasani, K. Nishio, M. Fukuoka, M. Varella-Garcia, K. Nakagawa, P. A. Jänne, Activation of ERBB2 signaling causes resistance to the EGFR-directed therapeutic

antibody cetuximab. Sci Transl Med 3, 99ra86 (2011)

26. E. Valtorta, S. Misale, A. Sartore-Bianchi, I. D. Nagtegaal, F. Paraf, C. Lauricella, V. Dimartino, S. Hobor, B. Jacobs, C. Ercolani, S. Lamba, E. Scala, S. Veronese, P. Laurent-Puig, S. Siena, S. Tejpar, M. Mottolese, C. J. Punt, M. Gambacorta, A. Bardelli, F. Di Nicolantonio, KRAS gene amplification in colorectal cancer and impact on response to EGFR-targeted therapy. Int J Cancer, (2013)

27. A. Bardelli, S. Corso, A. Bertotti, S. Hobor, E. Valtorta, G. Siravegna, A. Sartore-Bianchi, E. Scala, A. Cassingena, D. Zecchin, M. Apicella, G. Migliardi, F. Galimi, C. Lauricella, C. Zanon, T. Perera, S. Veronese, G. Corti, A. Amatu, M. Gambacorta, L. A. Diaz, M. Sausen, V. E. Velculescu, P. Comoglio, L. Trusolino, F. Di Nicolantonio, S. Giordano, S. Siena, Amplification of the MET Receptor Drives Resistance to Anti-EGFR Therapies in Colorectal Cancer. Cancer Discov 3, 658-673 (2013)

28. M. Janakiraman, E. Vakiani, Z. Zeng, C. A. Pratilas, B. S. Taylor, D. Chitale, E. Halilovic, M. Wilson, K. Huberman, J. C. Ricarte Filho, Y. Persaud, D. A. Levine, J. A. Fagin, S. C. Jhanwar, J. M. Mariadason, A. Lash, M. Ladanyi, L. B. Saltz, A. Heguy, P. B. Paty, D. B. Solit, Genomic and biological characterization of exon 4 KRAS mutations in human cancer. Cancer Res 70, 5901-5911 (2010)

29. F. Morgillo, T. Cascone, E. D'Aiuto, E. Martinelli, T. Troiani, P. Saintigny, R. De Palma, J. V. Heymach, L. Berrino, C. Tuccillo, F. Ciardiello, Antitumour efficacy of MEK inhibitors in human lung cancer cells and their derivatives with acquired resistance to different tyrosine kinase inhibitors. Br J Cancer 105, 382-392 (2011)

30. A. Akinleye, M. Furqan, N. Mukhi, P. Ravella, D. Liu, MEK and the inhibitors: from bench to bedside. J Hematol Oncol 6, 27 (2013)

31. M. J. Overman, J. Modak, S. Kopetz, R. Murthy, J. C. Yao, M. E. Hicks, J. L. Abbruzzese, A. L. Tam, Use of research biopsies in clinical trials: are risks and benefits adequately discussed? J Clin Oncol 31, 17-22 (2013)

32. F. Diehl, K. Schmidt, M. A. Choti, K. Romans, S. Goodman, M. Li, K. Thornton, N. Agrawal, L. Sokoll, S. A. Szabo, K. W. Kinzler, B. Vogelstein, L. A. Diaz, Circulating mutant DNA to assess tumor dynamics. Nat Med 14, 985-990 (2008)

33. E. Crowley, F. Di Nicolantonio, F. Loupakis, A. Bardelli, Liquid biopsy: monitoring cancer-genetics in the blood. Nat Rev Clin Oncol 10, 472-484 (2013)

34. Bettegowda. C, Circulating tumor DNA for the detection and monitoring of human malignancies. Science Translational Medicine, (2014).

35. S. D. Markowitz, M. M. Bertagnolli, Molecular origins of cancer: Molecular basis of colorectal cancer. N Engl J Med 361, 2449-2460 (2009)

36. P. I. Poulikakos, Y. Persaud, M. Janakiraman, X. Kong, C. Ng, G. Moriceau, H. Shi, M. Atefi, B. Titz, M. T. Gabay, M. Salton, K. B. Dahlman, M. Tadi, J. A. Wargo, K. T. Flaherty, M. C. Kelley, T. Misteli, P. B. Chapman, J. A. Sosman, T. G. Graeber, A. Ribas, R. S. Lo, N. Rosen, D. B. Solit, RAF inhibitor resistance is mediated by dimerization of aberrantly spliced BRAF(V600E). Nature 480, 387-390 (2011)

37. J. G. Greger, S. D. Eastman, V. Zhang, M. R. Bleam, A. M. Hughes, K. N. Smitheman, S. H. Dickerson, S. G. Laquerre, L. Liu, T. M. Gilmer, Combinations of BRAF, MEK, and PI3K/mTOR inhibitors overcome acquired resistance to the BRAF inhibitor GSK2118436 dabrafenib, mediated by NRAS or MEK mutations. Mol Cancer Ther 11, 909-920 (2012)

38. K. T. Flaherty, J. R. Infante, A. Daud, R. Gonzalez, R. F. Kefford, J. Sosman, O. Hamid, L. Schuchter, J. Cebon, N. Ibrahim, R. Kudchadkar, H. A. Burris, G. Falchook, A. Algazi, K. Lewis, G. V. Long, I. Puzanov, P. Lebowitz, A. Singh, S. Little, P. Sun, A. Allred, D. Ouellet, K. B. Kim, K. Patel, J. Weber, Combined BRAF and MEK inhibition in melanoma with BRAF V600 mutations. N Engl J Med 367, 1694-1703 (2012)

39. A. Prahallad, C. Sun, S. Huang, F. Di Nicolantonio, R. Salazar, D. Zecchin, R. L. Beijersbergen, A. Bardelli, R. Bernards, Unresponsiveness of colon cancer to BRAF(V600E) inhibition through feedback activation of EGFR. Nature, (2012)

40. M. S. Edwards, S. D. Chadda, Z. Zhao, B. L. Barber, D. P. Sykes, A systematic review of treatment guidelines for metastatic colorectal cancer. Colorectal Dis 14, e31-47 (2012)

41. N. E. Kemeny, Treatment of metastatic colon cancer: "the times they are A-changing". J Clin Oncol 31, 1913-1916 (2013)

42.   R. H. Whitehead, F. A. Macrae, D. J. St John, J. Ma, A colon cancer cell line (LIM1215) derived from a patient with inherited nonpolyposis colorectal cancer. J Natl Cancer Inst 74, 759-765 (1985)

43.   F. Diehl, K. Schmidt, K. H. Durkee, K. J. Moore, S. N. Goodman, A. P. Shuber, K. W. Kinzler, B. Vogelstein, Analysis of mutations in DNA isolated from plasma and stool of colorectal cancer patients. Gastroenterology 135, 489-498 (2008)

44.   A. I. Roig, U. Eskiocak, S. K. Hight, S. B. Kim, O. Delgado, R. F. Souza, S. J. Spechler, W. E. Wright, J. W. Shay, Immortalized epithelial cells derived from human colon biopsies express stem cell markers and differentiate in vitro. Gastroenterology 138, 1012-1021.e1011-1015 (2010)

45.   C. J. Lord, S. McDonald, S. Swift, N. C. Turner, A. Ashworth, A high-throughput RNA interference screen for DNA repair determinants of PARP inhibitor sensitivity. DNA Repair (Amst) 7, 2010-2019 (2008)

Acknowledgements

Funding

Author contributions

AB, FDN and SM designed the study; FDN and AB devised the MEK-EGFR combinatorial treatment; AB conceived the idea of monitoring genetic alterations in patients' blood. AS-B, KB, AA and SS identified and provided clinical data on patients treated with anti-EGFR monoclonal antibodies. SM, SA, SL, GS, AL, SH, MR, MB, LL, CL and EV generated and analyzed laboratory-based data; AB, FDN and SM wrote the manuscript. All authors revised and approved the manuscript.

Competing interests

S.S. is a clinical investigator of MEK inhibitors for colorectal cancer for Bayer, GSK, and Novartis. A.S-B. is a member of the advisory board for Amgen and has received speaking fees from Amgen and Bayer. A.B. is a shareholder and board member of Horizon Discovery, Cambridge UK. A.B., F.DN. and

S.S. are co-inventors of a patent on "Methods of detecting and predicting acquired resistance to anti-EGFR treatment in colorectal cancer" (application number: 42823-502P01US). The other authors declare no competing interests.

Materials and data availability

LIM1215 can be obtained through MTA from the Ludwig Institute for Cancer Research, Zurich, Switzerland. HCA-46 are commercially available from the European Collection of Cell Cultures (ECACC cat no.07031601). The NCIH508 are commercially available from the American Type Culture Collection (catalog no. ATCC CCL-253). The DiFi and OXCO-2 cell lines were a kind gift from Dr J. Baselga in November 2004 (Oncology Department of Vall d'Hebron University Hospital, Barcelona, Spain) and Dr V. Cerundolo in March 2010 (Weatherall Institute of Molecular Medicine, University of Oxford, UK), respectively. Both cell lines can be obtained from the corresponding author.

Figure legends

Figure 1: CRC cell lines resistant to cetuximab or panitumumab carry KRAS, NRAS or BRAF mutations. (A) DiFi, HCA-46, LIM1215, NCIH508 and OXCO-2 cetuximab (R-cetux) and panitumumab (R-panit) resistant cells were treated with cetuximab (Cmab, in black) or with panitumumab (Pmab, in grey) for one week, with increasing concentrations of the two drugs. Parental cells treated with cetuximab (red circles) or with panitumumab (red triangles) were included as controls. The name of the EGFR-targeted monoclonal antibody (anti-EGFR moAB) employed in each viability assay is indicated in parentheses. Cell viability was measured by the ATP assay. Data points represent means ± SD of three independent experiments. (B) List of genes and molecular alterations detected in cetuximab and panitumumab resistant derivatives. LIM1215 R1- and R4-cetux, LIM1215 R-panit, NCIH508 R-panit, OXCO-2 R1-cetux, OXCO-2 R2-cetux and OXCO-2 R-panit contain multiple mutations in the same cell population. The nomenclature -R1 -R2 -R3 -R4 indicate cetuximab resistant populations, independently derived from the parental cell line.

Figure 2: Genetic alterations in the EGFR signaling cascade biochemically converge to activate MEK and ERK. The indicated cell lines were analyzed for EGFR-MAPK pathway activation. Parental and resistant cells were treated with cetuximab (Cmab, 1.4 µM) or panitumumab (Pmab, 1.4 µM), after which whole-cell extracts were subjected to Western blot analysis and compared to untreated cells with phospho-EGFR (Tyr 1068), total EGFR, total MEK1/2 and phospho-MEK1/2, total ERK1/2 and phospho-ERK1/2 antibodies. Vinculin was included as a loading control. The genetic status of the resistant derivatives is listed below the blots.

Figure 3: Cell lines with acquired resistance to anti-EGFR antibodies are sensitive to suppression of EGFR and MEK1/2. (A) siRNA suppression screening of genes involved in the EGFR pathway was performed using the indicated cell lines. The genetic status of the individual cell models is shown below the graph. Effective impairment of cell proliferation was arbitrarily set at less than 50% (dashed line). The survival fraction was determined by ATP assay. Data points represent means ± SD of three independent experiments. (Black: HER family receptors; Red: Ras family members; Grey: Ras downstream effectors). (B) Dual silencing of EGFR together with individual EGFR pathway effectors. Effective impairment of cell proliferation was arbitrarily set at less than 50% (dashed line). The survival fraction was assayed by the ATP assay. Data points represent means ± SD of three independent experiments (Black: combination of EGFR+RAS effectors; Grey: combination of KRAS+BRAF; Red: combination of KRAS+MEK-1/2).

Figure 4: MEK inhibition induces EGFR activation, resulting in ERK activation. Resistant cells were treated with pimasertib (50 nM) with or without cetuximab (340 nM) at the indicated time points, after which whole-cell extracts were subjected to Western blot analysis. Whole-cell extracts were blotted with phospho-EGFR (Tyr1068), total EGFR, phospho-MEK1/2, total MEK1/2, phospho-ERK and total ERK. Actin was included as a loading control. NT: not treated.

Figure 5: Resistance to EGFR therapy is reversed by pharmacological inhibition of EGFR and MEK. (A) The indicated cell lines were treated for two weeks with increasing concentrations of cetuximab and pimasertib. At the end of the assay, cells were fixed and stained with crystal violet solution. The genetic status of each individual cell model is indicated. NT: not treated. (B) Combinatorial treatment with cetuximab plus pimasertib is effective in inducing tumor shrinkage in vivo. OXCO-2 R1-cetux and NCIH508 R-cetux were injected subcutaneously in nude mice and then treated with cetuximab or pimasertib as monotherapy, with the combination of the two drugs, or with vehicle. N=7 mice per group for OXCO-2 R1-cetux and 4 mice per group for NCIH508 R-cetux.

Figure 6: Circulating DNA in patients resistant to anti-EGFR therapy displays KRAS and NRAS mutations. (A-C) BEAMing analysis of circulating tumor DNA of four patients with acquired resistance to cetuximab (patient #1) or panitumumab (patients #2, #3, #4) displays complex patterns of KRAS and NRAS mutations. (D-E) Mouse xenografts from a tumor at relapse after anti-EGFR therapy respond to combined EGFR-MEK inhibition. (D) Xenografted tumors retained the histopathologic characteristics of original samples. Hematoxylin and eosin stains of the biopsy taken from the original colorectal cancer lung metastasis and a histological sample derived from the same lesion engrafted in a NOD-SCID mouse. Scale bar, 50 μm. (E) Waterfall plot showing the percent change in volume for the individual tumors in each arm at the time of sacrifice. Tumor volumes were normalized individually to their volumes at treatment day 1.

A

DiFi

cell viability (fold control)

anti-EGFR moABs [M]

HCA-46

cell viability (fold control)

anti-EGFR moABs [M]

LIM1215

cell viability (fold control)

anti-EGFR moABs [M]

NCIH508

cell viability (fold control)

anti-EGFR moABs [M]

OXCO-2

cell viability (fold control)

anti-EGFR moABs [M]

- Parental (Cmab)
- Parental (Pmab)
- R1-cetux (Cmab)
- R2-cetux (Cmab)
- R-panit (Cmab)
- R1-cetux (Pmab)
- R2-cetux (Pmab)
- R-panit (Pmab)

B

Cetuximab resistant derivative	Genetic alterations at resistance
DiFi R-cetux	KRAS amplification
HCA-46 R1-cetux	KRAS amplification
HCA-46 R2-cetux	KRAS p.G13D
LIM1215 R1-cetux	KRAS p.G12R, KRAS p.K117N and NRAS p.G12C
LIM1215 R2-cetux	KRAS p.G13D
LIM1215 R3-cetux	KRAS p.A146T
LIM1215 R4-cetux	KRAS p.G12D and KRAS p.G13D
NCIH508 R-cetux	KRAS amplification
OXCO-2 R1-cetux	KRAS p.G12D and BRAF p.V600E
OXCO-2 R2-cetux	NRAS p.G12C, NRAS p.G12D and NRAS p.G13D
Panitumumab resistant derivative	Genetic alterations at resistance
DiFi R-panit	KRAS p.G12D
HCA-46 R-panit	KRAS p.G12C
LIM1215 R-panit	KRAS p.G13D and NRAS p.G12C
NCIH508 R-panit	KRAS amplification and NRAS p.G12C
OXCO-2 R-panit	KRAS p.G12D and NRAS p.Q61R

A LIM1215

Parental   Resistant
Pmab   -   +   -   +

pEGFR
Y1068
EGFR
pMEK
MEK
pERK
ERK
Vinculin

LIM1215 R-panit:
KRAS G13D/NRAS G12C

B OXCO -2

Parental   Resistant
Cmab   -   +   -   +

pEGFR
Y1068
EGFR
pMEK
MEK
pERK
ERK
Vinculin

OXCO-2 R1-cetux:
KRAS G12D/BRAF V600E

C HCA -46

Parental   Resistant
Pmab   -   +   -   +

pEGFR
Y1068
EGFR
pMEK
MEK
pERK
ERK
Vinculin

HCA-46 R-panit:
KRAS G12C

D NCIH508

Parental   Resistant
Cmab   -   +   -   +

pEGFR
Y1068
EGFR
pMEK
MEK
pERK
ERK
Vinculin

NCIH508 R-cetux:
KRAS Amplified

LIM1215 R-panit
(KRASG13D/NRAS G12C)

Pimasertib

Pimasertib+Cmab

NT 1h 3h 6h 12h 1h 3h 6h 12h

p-EGFR
Y1068

EGFR

p-MEK

MEK

p-ERK

ERK

Actin

OXCO-2 R1-cetux
(KRAS G12D/BRAF V600E)

Pimasertib

Pimasertib+Cmab

NT 1h 3h 6h 12h 1h 3h 6h 12h

p-EGFR
Y1068

EGFR

p-MEK

MEK

p-ERK

ERK

Actin

HCA-46 R-panit
(KRAS G12C)

Pimasertib

Pimasertib+Cmab

NT 1h 3h 6h 12h 1h 3h 6h 12h

p-EGFR
Y1068

EGFR

p-MEK

MEK

p-ERK

ERK

Actin

NCIH508 R-cetux
(KRAS Amplified)

Pimasertib

Pimasertib+Cmab

NT 1h 3h 6h 12h 1h 3h 6h 12h

p-EGFR
Y1068

EGFR

p-MEK

MEK

p-ERK

ERK

Actin

A
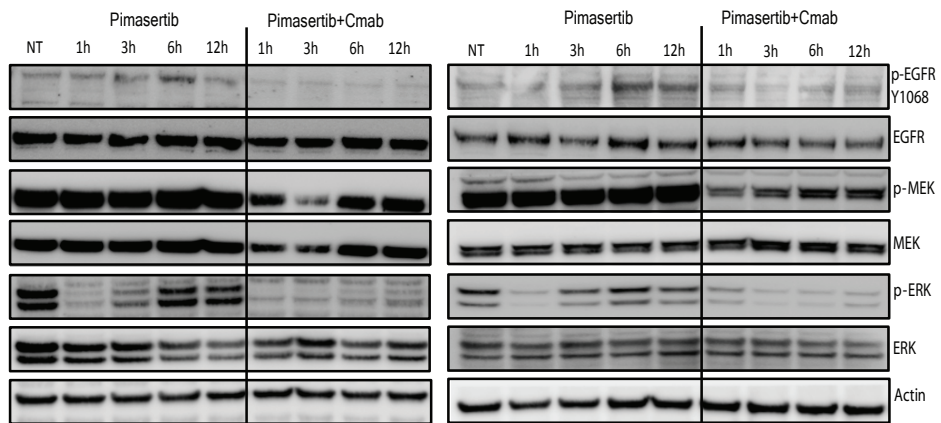
LIM1215 R-panit
KRAS G13D/NRAS G12C
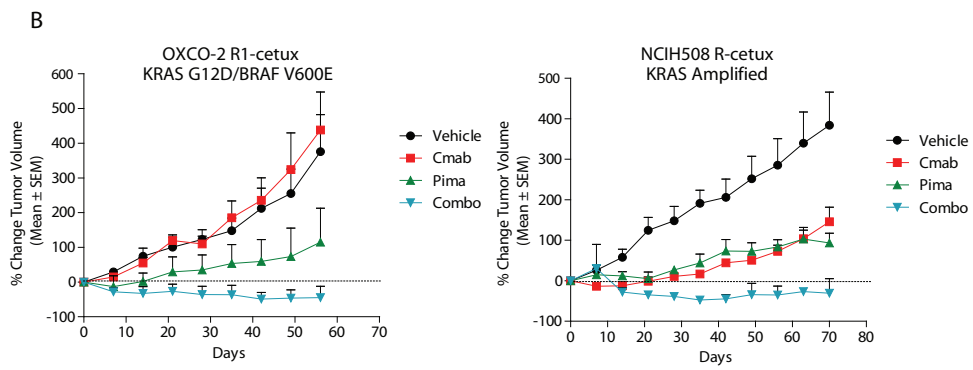
OXCO-2 R1-cetux
KRAS G12D/BRAF V600E

HCA-46 R-panit
KRAS G12C

NCIH508 R-cetux
KRAS Amplified

B

OXCO-2 R1-cetux
KRAS G12D/BRAF V600E

NCIH508 R-cetux
KRAS Amplified

% Change Tumor Volume (Mean ± SEM)

Days

- Vehicle
- Cmab
- Pima
- Combo

A Patient #1

B Patient #2

C

KRAS G13D

KRAS G12D

Baseline   Relapse

KRAS G12A

KRAS G12D
NRAS Q61H

KRAS G13D

KRAS G12D

Baseline   Relapse

% Mutated Alleles

NRAS G13R
KRAS G12A
NRAS Q61L

Relapse Patient #3   Relapse Patient #4

● KRAS G12A
● KRAS G12C
● KRAS G12D
● KRAS G12R
● KRAS G12S
● KRAS G12V
● KRAS G13D

■ NRAS Q61H
■ NRAS Q61L
■ NRAS Q61R

▲ NRAS G12C
▲ NRAS G12D
▲ NRAS G12S
▲ NRAS G13D
▲ NRAS G13R

◆ BRAF V600E

D

Lung metastasis at relapse after cetuximab   Patient derived xenograft

E

% of tumor growth after 6 weeks of treatment

Supplementary Materials and Methods

Cell culture and generation of resistant cells

DiFi cells were cultured in F12 medium (Invitrogen) supplemented with 5% FBS; LIM1215 cells were cultured in RPMI-1640 medium (Invitrogen) supplemented with 5% FBS and insulin (1 µg/ml); OXCO-2 cells were cultured in Iscove's medium (Invitrogen) supplemented with 5% FBS; NCIH508 cells were cultured in RPMI-1640 medium (Invitrogen) supplemented with 5% FBS, and HCA-46 cells were cultured in DMEM medium (Invitrogen) supplemented with 5% FBS. The generation of DiFi and LIM1215 cetuximab-resistant derivatives is described elsewhere (18). OXCO-2, NCIH508 and HCA-46 cetuximab-resistant derivatives were generated after 3-9 months of continuous exposure to the drug at a concentration of 0.3 µM for NCIH508 and 1.4 µM for OXCO-2 and HCA-46. LIM1215, DiFi, OXCO-2 and HCA-46 panitumumab-resistant derivatives were generated by 3-9 months of continuous exposure to the drug at a constant concentration of 1.4 µM. The NCIH508 cell line was purchased from American Type Culture Collection (LGC Standards Srl). The HCA-46 cell line was obtained from ECACC (distributed by Sigma-Aldrich Srl). The DiFi and OXCO-2 cell lines were a kind gift from Dr. J. Baselga in November 2004 (Oncology Department of Vall d'Hebron University Hospital, Barcelona, Spain) and Dr V. Cerundolo in March 2010 (Weatherall Institute of Molecular Medicine, University of Oxford, UK), respectively. The LIM1215 parental cell line has been described previously (*41*) and was obtained from Prof. Robert Whitehead, Vanderbilt University, Nashville, with permission from the Ludwig Institute for Cancer Research, Zurich, Switzerland. The genetic identity of the cell lines used in this study was confirmed by STR profiling (Cell ID, Promega).

Drug assays

Cetuximab and panitumumab were obtained from the Pharmacy at Niguarda Ca' Granda Hospital, Milan, Italy. Pimasertib was purchased from Selleck Chemicals. Cell lines were seeded in 100 µL medium at the following densities ($2x10^3$ for DiFi and $1.5 x10^3$ for LIM1215, HCA-46, NCIH508 and OXCO-2) in 96-well culture plates. After serial dilutions, drugs in serum-free medium were added to cells, and medium-only wells were included as controls. Plates were incubated at 37°C in 5% CO_2 for 6 days, after which cell viability was assessed by ATP content using the

CellTiter-Glo® Luminescent Assay (Promega). For long-term proliferation assays, cells were seeded in 24-well plates (5 x10^3 cells per well) and cultured in the absence and presence of drugs as indicated. Wells were fixed with 3% paraformaldehyde and stained with 1% Crystal Violet-Methanol solution (Sigma-Aldrich) after two weeks. All assays were performed independently at least three times.

Mutational analysis

For Sanger Sequencing, all samples were subjected to automated sequencing by ABI PRISM 3730 (Applied Biosystems). Primer sequences are listed in supplementary materials as table S3. The following genes and exons were analyzed: KRAS (exons 2, 3 and 4), NRAS (exons 2 and 3), HRAS (exons 2 and 3), PIK3CA (exons 9 and 20), BRAF (exon 15), EGFR (ectodomain). All mutations were confirmed twice, starting from independent PCR reactions.

BEAMing procedure

The BEAMing procedure is based on the initial description (*42*) with further optimizations in our laboratory as described below. DNA was extracted from plasma using the QIAamp Circulating Nucleic Acid Kit (QIAGEN) according to the manufacturer's instructions. BEAMing was performed as described previously (18). The first amplification was performed in a 50-µL PCR reaction containing DNA isolated from 1 ml of plasma, 1X Phusion high-fidelity buffer, 1.5 U of Hotstart Phusion polymerase (NEB, BioLabs), 0.5 µM of each primer with tag sequence, 0.2 mM of each deoxynucleoside triphosphate, and 0.5 mM MgCl$_2$. Amplification was carried out using the following cycling conditions: 98°C for 45 sec; 2 cycles of 98°C for 10 sec, 67°C for 10 sec, 72°C for 10 sec; 2 cycles of 98°C for 10 sec, 64°C for 10 sec, 72°C for 10 sec; 2 cycles of 98°C for 10 sec, 61°C for 10 sec, 72°C for 10 sec; 31 cycles of 98°C for 10 sec, 58°C for 10 sec, 72°C for 10 sec. PCR products were diluted and quantified using the PicoGreen double-stranded DNA assay (Invitrogen). A clonal bead population was generated by performing an emulsion PCR (emPCR).

A 150 µl PCR mixture was prepared containing 18 pg template DNA, 40 U of Platinum Taq DNA polymerase (Invitrogen), 1X Platinum buffer, 0.2 mM dNTPs, 5 mM MgCl$_2$, 0.05 µM Tag1 (tcccgcgaaattaatacgac), 8 µM Tag2 (gctggagctctgcagcta) and 6×10^7 magnetic streptavidin beads (MyOne, Invitrogen) coated with Tag1 oligonucleotide (dual biotin-TSpacer18-tcccgcgaaattaatacgac). The 150 µl PCR reactions were distributed into the wells of a 96-well PCR plate together with 70 µl of the Emulsifier oil (7% ABIL WE09-EVONIK, 73% Tegosoft DEC-EVONIK, 20% Mineral oil PCR reagent-SIGMA).The water-in-oil emulsion was obtained by pipetting. The PCR cycling conditions were: 94°C for 2 min; 50 cycles of 94°C for 10 sec, 58°C for 15 sec, 70°C for 15 sec. All primer and probe sequences are listed in supplementary materials as table S4.

Gene copy number analysis qPCR

Parental and resistant cell lines were trypsinized, washed with PBS and centrifuged; pellets were lysed and DNA was extracted using Wizard SV Genomic kit (Promega) according to the manufacturer's directions. Real time PCR was performed with 30 ng of DNA per single reaction using GoTaq QPCR Master Mix (Promega) with an ABI PRISM® 7900HT apparatus (Applied Biosytems). Sample analysis was normalized to a control diploid cell line, HCEC (*43*). All primer sequences are listed in supplementary materials as table S5.

siRNA screening

The siRNA targeting reagents were purchased from Dharmacon, as a SMARTpool of four distinct siRNA species targeting different sequences of the target transcript. The list of siRNAs is shown in Table S6. Cell lines were grown and transfected with SMARTpool siRNAs using Dharmafect 4 (DF4) (Dharmacon), Lipofectamine 2000 or RNAiMAX (Invitrogen). Each plate included the following controls: mock control (transfection lipid only), siControl Pool1 (Dharmacon), all Stars reagent (Qiagen) as negative control; Polo-like Kinase 1 (PLK1) (Dharmacon) served as a positive control. RNAi screening conditions were as described (*44*). After five days, cell viability in each well was estimated with a luminescent assay measuring cellular ATP levels (CellTiter-Glo® Luminescent Assay (Promega).

Immunoblot analysis

Prior to biochemical analysis, all cells were grown in their specific media supplemented with 5% FBS. Total cellular proteins were extracted by solubilizing the cells in boiling SDS buffer (50 mM Tris-HCl, pH 7.5, 150 mM NaCl, and 1% SDS) or in cold EB buffer (50 mM Hepes pH 7.4, 150 mM NaCl, 1% Triton X-100, 10% glycerol, 5 mM EDTA, 2 mM EGTA; all reagents were from Sigma-Aldrich, except for Triton X-100 from Fluka) in the presence of 1 mM sodium orthovanadate, 100 mM sodium fluoride and a mixture of protease inhibitors (pepstatin, leupeptin, aprotinin, STI and phenylmethylsulfonyl fluoride). Extracts were clarified by centrifugation, and protein concentration was determined using BCA protein assay reagent kit (Thermo). Western blot detection was performed with enhanced chemiluminescence system (GE Healthcare) and peroxidase conjugated secondary antibodies (Amersham). The following primary antibodies were used for western blotting (all from Cell Signaling Technology, except where indicated): anti-phospho- p44/42 ERK (thr202/tyr204); anti-p44/42 ERK; anti-phospho-MEK1/2 (Ser217/221), anti-MEK1/2; anti-KRAS (Santa Cruz); anti-EGFR (clone13G8, Enzo Life Sciences); anti-phospho EGFR (tyr1068); anti-actin and anti-vinculin (Sigma-Aldrich).

Ras activation assay

GST-RAF1-RAS binding domain fusion proteins were expressed in Escherichia coli by induction with 0.2 mM isopropyl-1-thioβ-D-galactopyranoside (IPTG) for 4 h at 30°C. The expressed fusion proteins were isolated from bacterial lysates by affinity chromatography with glutathione agarose beads. 600 μg of whole-cell cleared lysate was incubated with 10 μg of GST-RAF CRIB (cdc42 and Rac-interactive binding) for 90 min at 4°C. The complexes were collected by centrifugation and washed three times with lysis buffer. Proteins were separated by SDS-PAGE followed by Western blot. The KRAS protein was detected with Anti-K-Ras mAb (Abnova clone 3B10-2F2, cat. H00003845-M01). Total lysates (20 μg) from the above cells were immunoblotted with anti-vinculin antibody (Sigma-Aldrich) as a loading control.

Xenograft studies

All animals were manipulated according to protocols approved by the Ethical Commission of the Institute for Cancer Research and Treatment and by the Italian

Ministry of Health. All experiments were performed in accordance with relevant local and national guidelines and regulations. Ten million NCIH508 R-cetux and OXCO-2 R-cetux cells were injected subcutaneously into the right posterior flank of 7-week-old CD-1 Nude Mice (Charles River Laboratories). When tumors reached an approximate volume of 400-450 mm^3, mice were randomized into 4 groups (7 mice each for OXCO-2 R1-cetux and 4 mice each for NCIH508 R-cetux) and treated with vehicle alone, cetuximab, pimasertib, or the combination of both drugs. Caliper measurements were taken once a week. Cetuximab was given by intraperitoneal injection at 0.5 mg/kg twice a week, and pimasertib was administered by gavage at 50 mg/kg/day. Pimasertib was suspended in distilled sterile water containing 0.5% carboxymethylcellulose (Sigma Aldrich) and 0.25% Tween 80 (Sigma Aldrich).

Patients

Plasma samples from CRC patients treated with cetuximab or panitumumab were obtained from Ospedale Niguarda Ca' Granda, Milan, under the Institutional Review Board-approved study #1014/09. All patients provided written informed consent and received EGFR-targeted treatment in the chemorefractory setting as per label indication. Patient #1 received cetuximab and irinotecan, achieving RECIST partial response (liver metastases) lasting 10 months. Patient #2, #3 and #4 received panitumumab monotherapy, achieving RECIST partial response (liver metastases) lasting 7, 5 and 12 months, respectively.

Patient derived xenograft (PDX)

The patient was diagnosed with pT4bN1bM0 colorectal cancer in 2011 and subsequently underwent adjuvant FOLFOX, which was prematurely stopped after 3 cycles because of severe hematological, gastrointestinal and cutaneous toxicity due to the presence of the dihydropyrimidine dehydrogenase genotype IVS14+1GA, associated with impairment of enzyme function and thus poor tolerability to 5-fluorouracil. After 5 months from diagnosis, relapse of disease occurred in peritoneum, pelvis, liver, spleen and lungs, and therefore treatment with cetuximab in combination with irinotecan was started. The patient achieved RECIST partial response in all sites of disease, which was maintained up to 7 months, when progression of the tumor occurred at all sites. Tumor biopsy of a lung lesion displaying progression was then performed, and the specimens were used to screen for molecular alterations for clinical studies and to generate a tumor-derived xenograft

(xenopatient) through a protocol approved by the Institutional Review Board of Ospedale Niguarda Ca' Granda (194/2010). The metastatic lesion biopsy was cut into two pieces, and a fragment was implanted in a NOD-SCID mouse. After engraftment, the tumor was passaged and expanded for two generations until production of four cohorts, each consisting of 6 mice. These were randomized to vehicle alone, cetuximab monotherapy, pimasertib monotherapy, or their combination. Treatments started at week 3 and lasted six weeks. Animals receiving vehicle, cetuximab, or pimasertib alone had to be euthanized before six weeks for ethical reasons. Caliper measurements were taken once a week. Cetuximab was given by intraperitoneal injection at 0.5 mg/kg twice a week, and pimasertib was administered by gavage at 50 mg/kg/day. Pimasertib was resuspended in distilled sterile water containing 0.5% carboxymethylcellulose (Sigma Aldrich) and 0.25% Tween 80 (Sigma Aldrich).

Figure S1

A

	LIM1215	LIM1215 R-panit
KRAS	WT	p.G13D
NRAS	WT	p.G12C

B

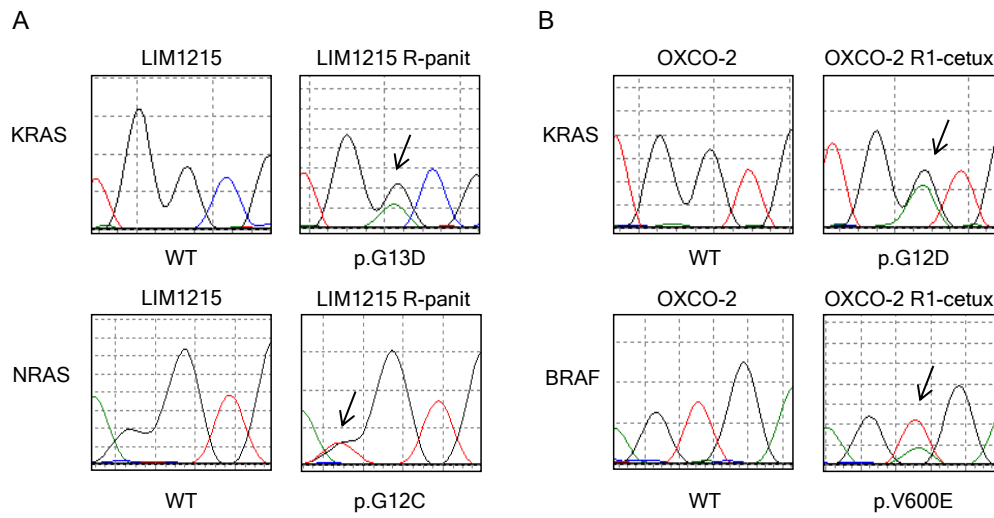|	OXCO-2	OXCO-2 R1-cetux
KRAS	WT	p.G12D
BRAF	WT	p.V600E

Figure S1: Mutational profiling of candidate genes in resistant cells. LIM1215 R-panit (A) and OXCO-2 R1-cetux (B) KRAS, NRAS and BRAF Sanger sequencing electropherograms revealed concomitant presence of KRAS and NRAS mutations in LIM1215 R-panit and concomitant KRAS and BRAF mutations in OXCO-2 R1-cetux.

Figure S2
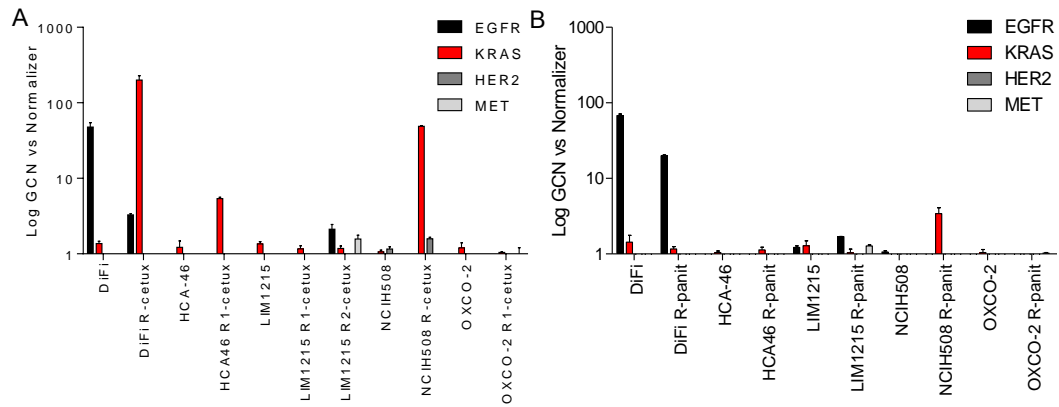
Figure S2: Gene copy number (GCN) analysis in resistant cells. Copy number of the EGFR, KRAS, HER2 and MET loci was determined by real-time quantitative PCR using gDNA extracted from DiFi, HCA-46, LIM1215, NCIH508 and OXCO-2 parental and cetuximab-resistant cells (A) or panitumumab-resistant cells (B). Primers designed to span centromeric regions of chromosomes 7, 12, and 17 were exploited to normalize data for aneuploidy. Genomic DNA from a diploid cell line (HCEC) was used as a reference control.

Figure S3
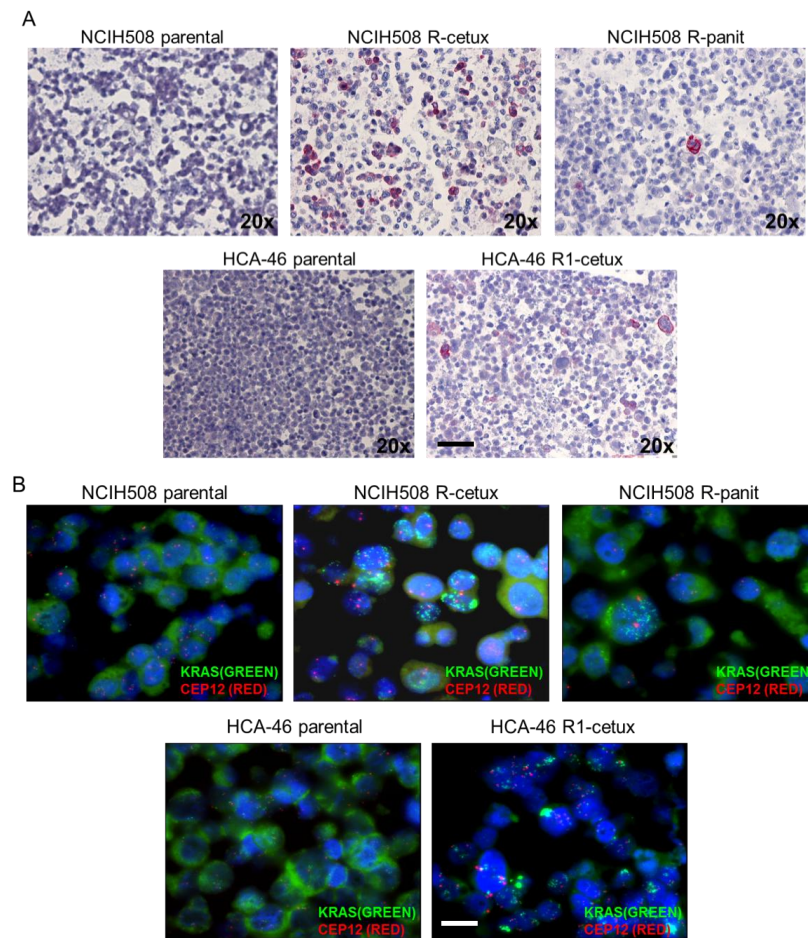
Figure S3: KRAS amplification in parental and resistant NCIH508 and HCA-46 cell lines.
(A) Immunohistochemical analysis of KRAS expression on cytoclots from NCIH508 and HCA46 parental and resistant cells. Scale bar, 50 μm. (B) FISH analysis of the KRAS gene on cytoclots from NCIH508 and HCA46 parental and resistant cells. The red signal represents the Chr12 centromeric probe (CEP12), which allows the determination of the total number of chromosome 12 in order to distinguish polisomy from real gene amplification; the green signal represents the KRAS gene probe. Scale bar, 10 μm.

Figure S4

Figure S4: Measurement of RAS activation in resistant cells. Active KRAS (GTP-KRAS) was assessed by GST-Raf1 pull-down in 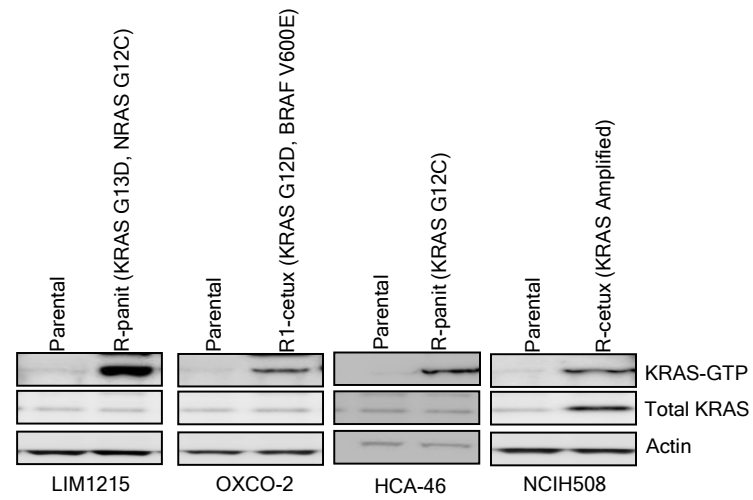LIM1215, OXCO-2, HCA-46 and NCIH508 parental and resistant cells. Whole-cell extracts were blotted with KRAS antibody. Actin is shown as a loading control.

Figure S5

A

**LIM1215 R-panit
(KRAS G13D/NRAS G12C)**

siRNA

NRAS KRAS MEK1-2 BRAF MOCK SCRAMBLE

— BRAF
— MEK1-2
— KRAS
— NRAS
— Actin

B

**LIM1215 R-panit
(KRAS G13D/NRAS G12C)**

siRNA

HRAS PIK3CA AKT CRAF EGFR HER2 HER3 SCRAMBLE

— EGFR
— HER2
— HER3
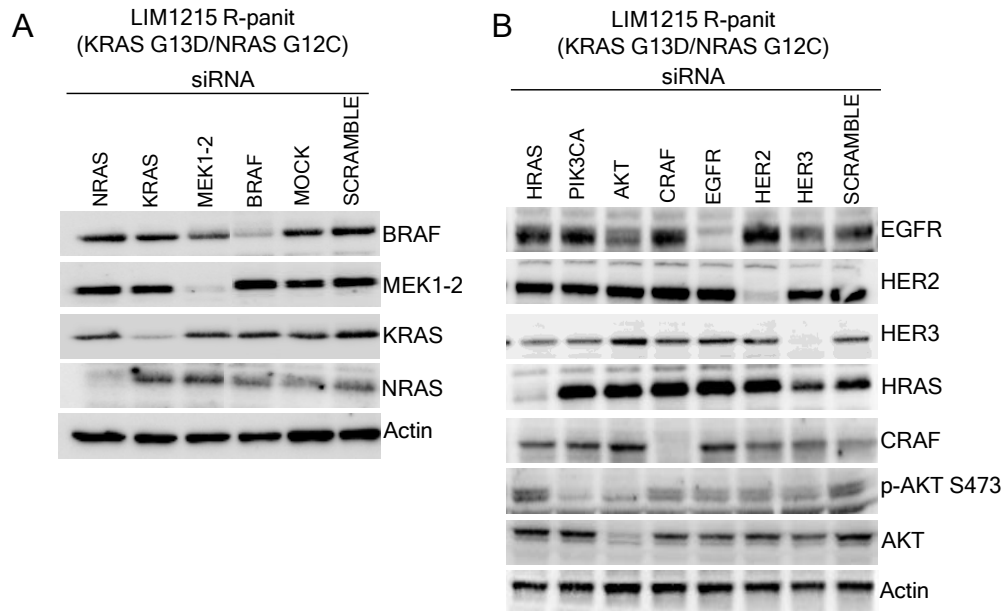— HRAS
— CRAF
— p-AKT S473
— AKT
— Actin

Figure S5: Biochemical validation of siRNA mediated gene knockdown. (A) LIM1215 R-panit were treated with siRNA targeting KRAS, NRAS, BRAF, and MEK1/2 for 72 hours, after which whole-cell extracts were subjected to western blot analysis. Whole-cell extracts were blotted with antibodies against BRAF, MEK1/2, KRAS, and NRAS. (B) LIM1215 R-panit cells were treated with siRNA for genes involved in EGFR signaling (EGFR, HER2, HER3, HRAS, CRAF, AKT, and PI3K) for 72 hours, after which whole-cell extracts were subjected to western blot analysis. Whole-cell extracts were blotted with antibodies against EGFR, HER2, HER3, HRAS, CRAF, and AKT. To evaluate PI3K knock down, we used phospho-AKT S473 as the main downstream effector. Actin was included as a loading control.

Figure S6
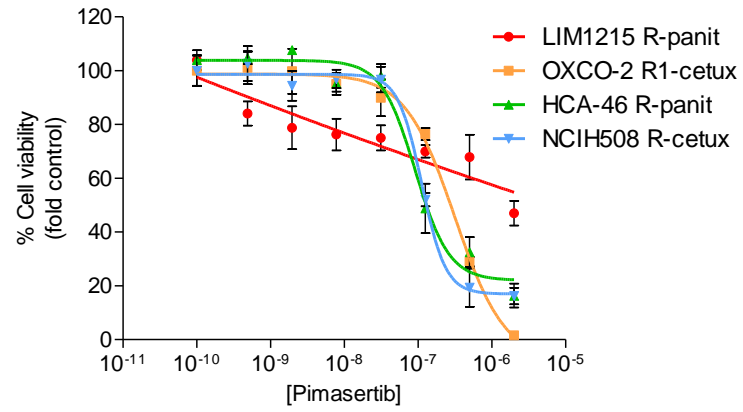
Figure S6: Pharmacological inhibition of MEK in cells resistant to anti-EGFR blockade. LIM1215 R-panit, OXCO-2 R1-cetux, HCA-46 R-panit, and NCIH508 R-cetux were treated with increasing concentrations of the MEK inhibitor pimasertib for one week. Cell viability was assayed by the ATP assay. Data points represent means ± SD of three independent experiments.

Figure S7
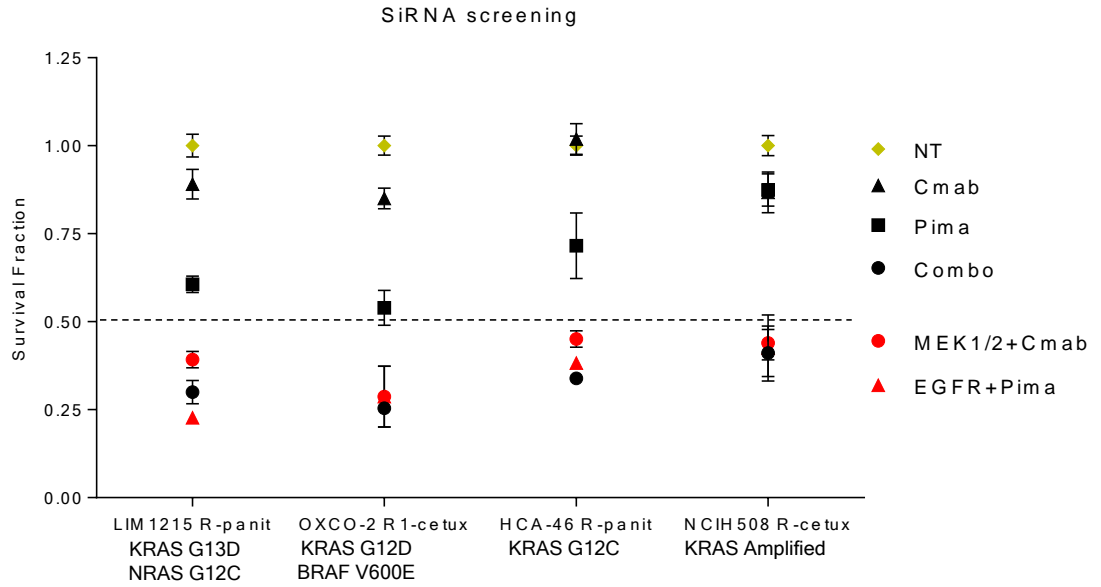
Figure S7: Pharmacological inhibition of EGFR or MEK1/2 with cetuximab or pimasertib. Silencing of EGFR or MEK1/2 (through siRNA) plus cetuximab or pimasertib in LIM1215 R-panit, OXCO-2 R1-cetux, HCA-46 R-panit and NCIH508 R-cetux cell lines is shown, together with the genetic status of the individual cell models. Cell lines treated with drugs alone are included as control. Survival fraction was assayed by the ATP assay. Data points represent means ± SD of three independent experiments. NT: not treated.

Figure S8
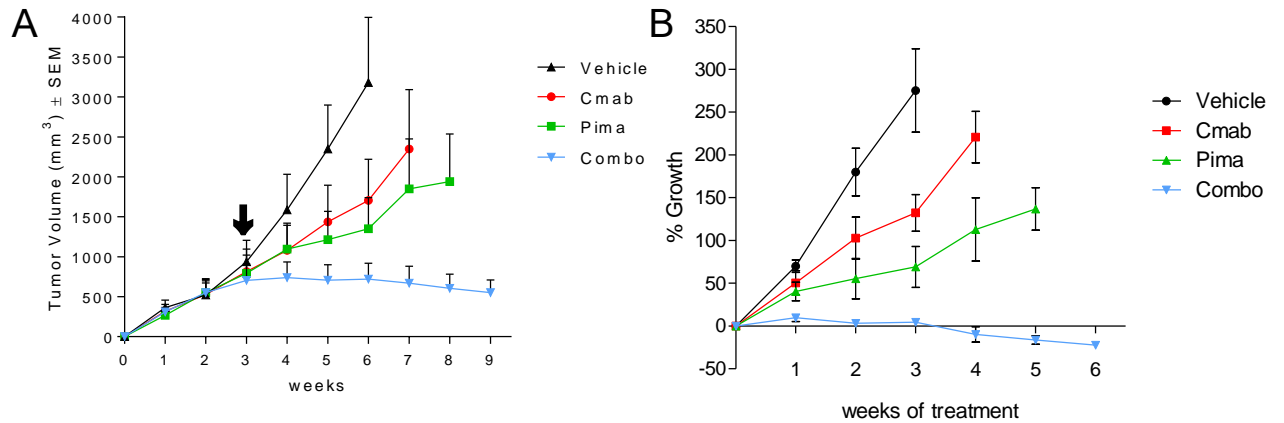
Figure S8: Sensitivity to combinatorial EGFR and MEK inhibition in a mouse xenograft from a metastatic CRC patient who relapsed after anti-EGFR therapy. (A) After engraftment in mouse, the tumor was serially transplanted for two generations until production of four cohorts, each consisting of 6 mice. These were randomized to vehicle alone, cetuximab monotherapy, pimasertib monotherapy, and their combination. Treatments started at week 3 (the arrow indicates the timepoint at which treatment was started) and lasted six weeks. Animals treated with vehicle, cetuximab, or pimasertib alone had to be euthanized before six weeks for ethical reasons. Tumor volumes are shown as mean±SEM (n=6 mice per group). (B) Percentage of tumor growth or shrinkage during treatment compared to tumor volume at treatment start for each individual mouse. Data points are shown as mean±SEM (n=6 mice per group).

Table S1

Cell lines	KRAS			BRAF	NRAS
	G12C	G12D	G13D	V600E	G12C
LIM1215 R-panit	0.00	0.00	17.78	0.00	0.52
HCA-46 R-panit	6.67	0.01	0.00	0.00	0.00
NCIH508 R-cetux	0.00	0.00	0.00	0.00	0.00
OXCO-2 R1-cetux	0.00	35.20	0.00	9.81	0.00

Supplementary Table 1: Frequencies of mutant alleles in resistant cell lines assessed by BEAMing. Genomic DNA extracted from resistant cell lines was analyzed with BEAMing probes for KRAS G12C, G12D, G13D, BRAF V600E, and NRAS G12C. Numbers represent the percentage of mutated alleles.

Table S3

Primer Name		gene/exon	sequence
F10	FORW	**BRAF ex15**	TGCTTGCTCTGATAGGAAAATG
F11	REV	**BRAF ex15**	AGCATCTCAGGGCCAAAAAT
F12	SEQ FOR	**BRAF ex15**	TGTTTTCCTTTACTTACTACACCTCA
225	FORW	**KRAS EX2**	GGTGGAGTATTTGATAGTGTATTAACC
226	REV	**KRAS EX2**	AGAATGGTCCTGCACCAGTAA
227	SEQ FOR	**KRAS EX2**	TCATTATTTTTATTATAAGGCCTGCTG
Krasex3_for	FORW	**KRAS EX3**	AAAGGTGCACTGTAATAATCCAGAC
Krasex3_rev	REV	**KRAS EX3**	ATGCATGGCATTAGCAAAGA
Krasex3_seq	SEQ FOR	**KRAS EX3**	CCAGACTGTGTTTCTCCCTTC
M04	FORW + SEQ	**KRAS EX4**	TGGACAGGTTTTGAAAGATATTTG
M05	REV	**KRAS EX4**	ATTAAGAAGCAATGCCCTCTCAAG
M18	FORW + SEQ	**NRAS exon2**	GTACTGTAGATGTGGCTCGC
M19	REV	**NRAS exon2**	AGAGACAGGATCAGGTCAGC
M29	FOR	**NRAS exon3**	CTTATTTAACCTTGGCAATAGCA
M22	REV + SEQ	**NRAS exon3**	GATTCAGAACACAAAGATCATCC
F16	FORW	**PI3K EX9**	GGGAAAAATATGACAAAGAAAGC
M17	REV	**PI3K EX9**	CTGCTTTATTTATTCCAATAGGTATGG
F18	SEQ FOR	**PI3K EX9**	TAGCTAGAGACAATGAATTAAGGGAAA
F19	FORW	**PI3K EX20**	CTCAATGATGCTTGGCTCTG
F20	REV	**PI3K EX20**	TGGAATCCAGAGTGAGCTTTC
F21	SEQ FOR	**PI3K EX20**	TTGATGACATTGCATACATTCG
M24	FORW	**HRAS exon2**	GGCAGGAGACCCTGTAGGA
M25	REV + SEQ	**HRAS exon2**	AGCCCTATCCTGGCTGTGT
M27	FORW + SEQ	**HRAS exon3**	AGAGGCTGGCTGTGTGAACT
M28	REV	**HRAS exon3**	ATGCGCAGAGAGGACAGGA
EGFR_ex12_ F	FORW	**EGFR ex12**	CCTCAAGGAGATAAGTGATGGAG
EGFR_ex12_R	REV	**EGFR ex12**	AAAGGACCCATTAGAACCAACTC

Supplementary Table 3: List of primers for gene amplification and sequencing

Table S4

PRIMER NAME	SEQUENCE	EXON
TAG1	TCCCGCGAAATTAATACGAC	
TAG2	GCTGGAGCTCTGCAGCTA	
TAG1 FOR BEADS	DUAL BIOTIN-T-SPACER18-TCCCGCGAAATTAATACGAC	
KRAS EX2 FOR	GCTGGAGCTCTGCAGCTATGACTGAATATAAACTTGTGGTAGTTG	KRAS EX 2
KRAS EX2 REV	TCCCGCGAAATTAATACGACCATATTCGTCCACAAAATGATTC	KRAS EX 2
KRAS EX3 FOR	GCTGGAGCTCTGCAGCTAAGACTGTGTTTCTCCCTTCTCAG	KRAS EX 3
KRAS EX3 REV	TCCCGCGAAATTAATACGACCTCATGTACTGGTCCCTCATTG	KRAS EX 3
KRAS EX4 FOR	GCTGGAGCTCTGCAGCTACAGGACTTAGCAAGAAGTTATGGA	KRAS EX 4
KRAS EX4 REV	TCCCGCGAAATTAATACGACGGACACTGGATTAAGAAGCAATG	KRAS EX 4
KRAS EX2 UNIVERSAL ALEXA 532	ALEXA 532-TGACGATACAGCTAATTCA	KRAS EX 2
KRAS 35 WILD-TYPE_ALEXA647	ALEXA647-GGAGCTGGTGGCGTA	KRAS EX 2
KRAS 38 WILD-TYPE_ALEXA647	ALEXA647-AGCTGGTGGCGTAGGC	KRAS EX 2
KRAS MUTANT 34GA_ALEXA488	ALEXA488-GGAGCTAGTGGCGTA	KRAS EX 2
KRAS MUTANT 34GC_ALEXA488	ALEXA488-GGAGCTCGTGGCGTA	KRAS EX 2
KRAS MUTANT 34GT_ALEXA488	ALEXA488-GGAGCTTGTGGCGTA	KRAS EX 2
KRAS MUTANT 35GA_ALEXA488	ALEXA488-GGAGCTGATGGCGTA	KRAS EX 2
KRAS MUTANT 35GC_ALEXA488	ALEXA488-GGAGCTGCTGGCGTA	KRAS EX 2
KRAS MUTANT 35GT_ALEXA488	ALEXA488-GGAGCTGTTGGCGTA	KRAS EX 2
KRAS MUTANT 38GA_ALEXA488	ALEXA488-AGCTGGTGACGTAGGC	KRAS EX 2
KRAS EX3 UNIVERSAL ALEXA532	ALEXA532-GGAAGCAAGTAGTAATTGA	KRAS EX 3
KRAS EX3 WT 183(61)_ALEXA647	ALEXA647-GCAGGTCAAGAGGAGT	KRAS EX 3
KRAS EX3 MUT 183AT(61)_ALEXA488	ALEXA488-GCAGGTCATGAGGAGT	KRAS EX 3
KRAS EX4 UNIVERSAL ALEXA532	ALEXA532-CAGGTAAGTAACACTGAA	KRAS EX 4
KRAS EX4 WT 436GA(146)_ALEXA647	ALEXA647-AACATCAGCAAAGACA	KRAS EX 4
KRAS EX4 MUT 436GA(146)_ALEXA488	ALEXA488-AACATCAACAAAGACA	KRAS EX 4
NRAS EX3 FOR	GCTGGAGCTCTGCAGCTACAAGTGGTTATAGATGGTGAAACC	NRAS EX 3
NRAS EX3 REV	TCCCGCGAAATTAATACGACTTATTGATGGCAAATACACAGAGG	NRAS EX 3
NRAS EX2 FOR	GCTGGAGCTCTGCAGCTAGGTTTCCAACAGGTTCTTGC	NRAS EX 2
NRAS EX2 REV	TCCCGCGAAATTAATACGACTGGTGGGATCATATTCATCTACA	NRAS EX 2
NRAS EXON3 UNIVERSAL_ALEXA532	ALEXA 532_GACCAATACATGAGGAC	NRAS EX 3
NRAS EXON3 WT (Q61_CAA)_ALEXA647	ALEXA 647_AGCTGGACAAGAAGAGT	NRAS EX 3
NRAS EXON3 MUT (Q61R_CGA)_ALEXA4	ALEXA 488_AGCTGGACGAGAAGAGT	NRAS EX 3
NRAS EX3 MUT (Q61H_183AT)_ALEXA48	ALEXA488-AGCTGGACATGAAGAGT	NRAS EX 3
NRAS EX3 MUT (Q61H_183AC)_ALEXA48	ALEXA488-AGCTGGACACGAAGAGT	NRAS EX 3
NRAS EX3 MUT (Q61L_182AT)_ALEXA48	ALEXA488-AGCTGGACTAGAAGAGT	NRAS EX 3
NRAS EXON2 UNIV (34-35)_ALEXA532	ALEXA532-AATGACTGAGTACAAACTG	NRAS EX 2
NRAS EX2 WT (34 & 35)_ALEXA 647	ALEXA647-GGTTGGAGCAGGTGGTGTTGG	NRAS EX 2
NRAS EX2 MUT (G12S_34GA)_ALEXA48	ALEXA488-GGTTGGAGCAAGTGGTGTTGG	NRAS EX 2
NRAS EX2 MUT (G12C_34GT)_ALEXA488	ALEXA488-GGTTGGAGCATGTGGTGTTGG	NRAS EX 2
NRAS EX2 MUT (G12D_35GA)_ALEXA48	ALEXA488-GGTTGGAGCAGATGGTGTTGG	NRAS EX 2
NRAS EX2 WT (37 & 38)_ALEXA 647	ALEXA647-TGGAGCAGGTGGTGTTGGGAA	NRAS EX 2
NRAS EX2 MUT (G13R_37GC)_ALEXA488	ALEXA488-TGGAGCAGGTCGTGTTGGGAA	NRAS EX 2
NRAS EX2 MUT (G13D_38GA)_ALEXA48	ALEXA488-TGGAGCAGGTGATGTTGGGAA	NRAS EX 2
BRAF EX15_FOR	GCTGGAGCTCTGCAGCTATCATAATGCTTGCTCTGATAGGA	BRAF EX15
BRAF EX15_REV	TCCCGCGAAATTAATACGACCCTCAATTCTTACCATCCACAAA	BRAF EX15
BRAF WT_T1799A_(V600E)_ALEXA647	ALEXA647-AGCTACAGTGAAATCTC	BRAF EX15
BRAF MUT_T1799A_(V600E)_ALEXA488	ALEXA488-AGCTACAGAGAAATCTC	BRAF EX15
BRAF UNIVERSAL_(V600E)_ TAMRA	TAMRA-ACTTACTACACCTCAGA	BRAF EX15
EGFR_EX12_1ST PCR F	GCTGGAGCTCTGCAGCTACCTCAAGGAGATAAGTGATGGAG	EGFR EX 12
EGFR_EX12_1ST PCR REV(2)	TCCCGCGAAATTAATACGACGACTTACTGCAGCTGTTTTCACC	EGFR EX 12
EGFR WT C1722C (S492R)_ALEXA647	ALEXA 647-ATTATAAGCAACAGAGGT	EGFR EX 12
EGFR MUT C1722A (S492R)_ALEXA488	ALEXA488-ATTATAAGAAACAGAGGT	EGFR EX 12
EGFR UNIVERSAL (S492R)_TAMRA	TAMRA-TTGTGCTATGCAAATACA	EGFR EX 12

Supplementary Table 4: List of primers and probes for BEAMing analysis

Table S5

Gene	Direction	Sequenza 5'-3' HUMAN
gEGFR F	Forward	TGGGCAACCCCGAGTATCT
gEGFR R	Reverse	CTAATTTGGTGGCTGCCTTTCT
gKRAS F	Forward	CTGAGCTCCCCAAATAGCTG
gKRAS R	Reverse	AGGTTAGGGCTAGGCACCAT
gMET F	Forward	TGTTTTAAGATCTGGGCAGTG
gMET R	Reverse	AATGTCACAACCCACTGAGG
gHER2 F	Forward	GTGAGTGATGGGGCTGAGTT
gHER2 R	Reverse	CCAGGGAGGAGTGAGTTGTC
gSTSG30022 chr7 F	Forward	CCTTCAAGAGAAAGACGACAG
gSTSG30022 chr7 R	Reverse	AGGACTTATAAAAGGCAAGGG
gD12S1595 chr12 F	Forward	GGGATCTTATGATGTGTCAGG
gD12S1595 chr12 R	Reverse	ACTCTTGGTCTCAGTCTGCC
ULK2_chr17 F	Forward	TTTGTGTGTGTGACGGAGTCT
ULK2_chr 17 R	Reverse	TTTGTGTGTGTGACGGAGTCT

Supplementary Table 5: List of primers for gene copy number analysis by real-time PCR

Table S6

GENE	PRODUCT NAME	CAT.NO
KRAS	siGENOME siRNA Reagents - Human	M-005069-00-0005
MAP2K1	siGENOME siRNA Reagents - Human	M-003571-01-0005
MAP2K2	siGENOME siRNA Reagents - Human	M-003573-03-0005
BRAF	siGENOME siRNA Reagents - Human	M-003460-03-0005
RAF1	siGENOME siRNA Reagents - Human	M-003601-02-0005
EGFR	siGENOME siRNA Reagents - Human	M-003114-03-0005
HER2	siGENOME siRNA Reagents - Human	M-003126-04-0005
HER3	siGENOME siRNA Reagents - Human	M-003127-03-0005
AKT1	siGENOME siRNA Reagents - Human	M-003000-03-0005
NRAS	siGENOME siRNA Reagents - Human	M-003919-00-0005
HRAS	siGENOME siRNA Reagents - Human	M-004142-00-0005
PI3K	siGENOME siRNA Reagents - Human	M-003201-04-0005

Supplementary Table 6: List of siRNA